Anat Embryol (1991) 184:225–243

Anatomy
and Embryology

The GABAergic cerebello-olivary projection in the rat*

Barbara J. Fredette and Enrico Mugnaini**

Laboratory of Neuromorphology, Box U-154, University of Connecticut, Storrs, CT 06269, USA

Accepted March 27, 1991

Summary. Immunocytochemical detection of glutamate decarboxylase (GAD), the predominant biosynthetic enzyme of gamma-aminobutyric acid (GABA), reveals the presence of a dense GABAergic innervation in all parts of the inferior olive. One brain center that provides a substantial projection to the inferior olive is the cerebellar nuclei, which contain many small GABAergic neurons. These neurons were tested as a source of GABAergic olivary afferents by combining retrograde tract tracing with GAD immunocytochemistry. As expected from previous studies, injections of wheat germ agglutinin-conjugated horseradish peroxidase (WGA-HRP) into the inferior olive retrogradely label many small neurons in the interposed and lateral cerebellar nuclei and the dorsal part of the lateral vestibular nucleus, and fewer neurons in the ventro-lateral region of the medial cerebellar nucleus. These projections are predominantly crossed and are topographically arranged. The vast majority, if not all, of these projection neurons are also GAD-positive. The relative contribution of this projection to the GABAergic innervation of the inferior olive was tested by lesion of the cerebellar nuclei, or the superior cerebellar peduncle. Within 10 days the lesion eliminates most GAD-immunoreactive boutons in the principal olive, the rostral lamella of the medial accessory olive, the ventrolateral outgrowth, and the lateral part of the dorsal accessory olive ventral fold. Thus, the effectiveness of this depletion demonstrates that the cerebellar nuclei provide most of the GABAergic innervation to regions of the inferior olive known to receive a cerebellar projection. Moreover, when the lateral vestibular nucleus is damaged, the dorsal fold of the dorsal accessory olive is depleted of GABAergic boutons. The synaptic relations that boutons of the GABAergic cerebello-olivary projection share with olivary neurons were investigated at the electron microscopic level by GAD-immunocytochemistry, anterograde degeneration of the cerebellar axons or anterograde transport of WGA-HRP. All of these methods confirm that GABAergic, cerebello-olivary axon terminals contain pleomorphic vesicles, and synapse on various portions of olivary neurons, and especially on dendritic spines within glomeruli, often in very close proximity to the gap junctions that characteristically couple the dendritic profiles. These results demonstrate four major points: that virtually all of the GABAergic, and presumably inhibitory, neurons of the cerebellar and dorsal lateral vestibular nuclei are projection neurons; that a large portion of the inferior olive receives GABAergic afferents from the cerebellar nuclei; that a portion of the dorsal accessory olive receives GABAergic afferents from the dorsal lateral vestibular nucleus; and that cerebello-olivary fibers often synapse near gap junctions, and therefore could influence electrical coupling of olivary neurons.

* This paper is dedicated to Professor Fred Walberg on the occasion of his 70th birthday.

** Formerly, Barbara J. Nelson; *present address:* Department of Physiology and Neurobiology, U-42, University of Connecticut, Storrs, CT 06269, USA

Offprint requests to: B.J. Fredette

Abbreviations. aMAO, subnucleus a of MAO; *beta,* beta nucleus; *bMAO,* subnucleus b of MAO; *cMAO,* subnucleus c of MAO; *dc* dorsal cap; *DC,* dorsal cochlear nucleus; *dfDAO,* dorsal fold of DAO; *dlh,* dorsal lateral hump of cerebellar nuclei; *dlPO,* dorsal lamella of PO; *Giα,* gigantocellular reticular nucleus; *dmcc,* dorsomedial cell column; *GABA,* gamma-aminobutyric acid; *GAD,* glutamate decarboxylase; *HRP,* horseradish peroxidase; *icp,* inferior cerebellar peduncle; *IC,* inferior colliculus; *Inf,* infracerebellar nucleus; *IntA,* anterior interposed cerebellar nucleus; *IntP,* posterior interposed cerebellar nucleus; *Lat,* lateral cerebellar nucleus; *LRt,* lateral reticular nucleus; *LSO,* lateral superior olive; *LVe,* lateral vestibular nucleus; *MAO,* medial accessory olive; *Med,* medial cerebellar nucleus; *Me5,* mesencephalic trigeminal nucleus; *MVe,* medial vestibular nucleus; *PFl,* paraflocculus of the cerebellar cortex; *PO,* principle olive; *RMg* raphe magnus; *rMAO,* rostral lamella of MAO; *rs,* rubrospinal tract; *scp,* superior cerebellar peduncle; *SpVe,* spinal vestibular nucleus; *SuVe,* superior vestibular nucleus; *vfDAO,* ventral fold of DAO; *vlo,* ventrolateral outgrowth; *vlPO,* ventral lamella of PO; *Y,* y vestibular nucleus; *WGA,* wheatgerm agglutinin

Key words: Inhibition – Cerebellar nuclei – Vestibular nuclei – Inferior olive – Glutamate decarboxylase

Introduction

Previous studies have demonstrated the presence of a dense but heterogeneous GABAergic innervation in the mammalian inferior olive (IO). GABAergic boutons in the principal olive (PO), the ventrolateral outgrowth, the rostral subdivisions of the medial accessory olive (MAO) and the dorsal accessory olive (DAO) can be differentiated from the GABAergic boutons in other olivary regions by their smaller size (Nelson and Mugnaini 1989; Nelson et al. 1989). These regions of the IO are connected to the cerebellar nuclei by reciprocal and topographically organized projections (reviewed by Dietrichs and Walberg 1989). Tract-tracing studies have determined that small neurons of the lateral and interposed cerebellar nuclei provide most, if not all, of the cerebello-olivary projection (Tolbert et al. 1976, 1978; Martin et al. 1976; Brown et al. 1977; Chan-Palay 1977; McCrea et al. 1978; Swenson and Castro 1983a; Legendre and Courville 1987). Immunocytochemical studies have thus far revealed the presence of two types of neurons in the cerebellar nuclei: small to medium size GABAergic neurons (Chan-Palay 1977, 1982; Mugnaini and Oertel 1981, 1985; Ottersen and Storm-Mathisen 1984; Monaghan et al. 1986a) and large neurons containing glutamate-like immunoreactivity (Monaghan et al. 1986b). The GABAergic neurons have been considered as local circuit neurons (Chan-Palay 1977), but McCrea et al. (1978) observed that nearly all the small neurons in the interposed nucleus are projection neurons. In the present study, we demonstrate, by combined GAD immunocytochemistry and retrograde tract-tracing, that the cerebello-olivary projection originates from small GABAergic neurons in the cerebellar nuclei, and that small GABAergic neurons in the lateral vestibular nucleus also project to the IO.

The portions of the IO that receive the cerebellar projection can be virtually depleted of GABAergic boutons by lesion of the cerebello-olivary pathway. GABA usually exerts an inhibitory effect on post-synaptic targets (Krnjevic 1976), and thus, our demonstration of a strong GABAergic projection from the deep nuclei is in contrast to the previously held tenet that all cerebellar nuclear output is excitatory. These results, presented elsewhere in preliminary form (Nelson et al. 1984; Nelson and Mugnaini 1985, 1989), confirm and extend other studies which have appeared on this subject after our original reports.

Materials and methods

Sprague-Dawley rats, 150–500 g in body weight, were used in this study. The animals were housed and handled according to recommended guidelines of the Public Health Service and monitored by the Institutional Animal Care and Use Committee at The University of Connecticut. All surgical and perfusion-fixation procedures were performed on rats under deep sodium pentobarbital anesthesia.

Double-labeling of cerebello-olivary neurons. Twenty-three rats received 10–100 nl injections of 2.5% or 5% WGA-HRP (type VI, Sigma Chemical Corp.) into the territory of the IO. A ventral approach was used to insert a glass micropipette into the brainstem (for details, see Brown et al. 1977). The tracer was pressure injected with a Picospritzer (General Valve Corp., Fairfield, New Jersey). After a 36–48 h survival, the rats were perfused transcardially with 200 ml of 0.9% NaCl, at 20° C, followed by 1,000 ml of a fixative solution containing 0.2% zinc salicylate, 4% formaldehyde and 0.94 NaCl, pH 6.5, 20° C. The brains were dissected out 1 h after termination of the perfusion, and immediately sectioned on a Vibratome (Oxford Laboratories) at 15–20 μm. Coronal serial sections were collected in three sets. One set of sections was processed for HRP histochemistry, by incubation for 15 min in 0.05% diaminobenzidine (DAB, Sigma), 0.02% cobalt hexachloride, 0.025% nickel ammonium sulfate, and 0.01% hydrogen peroxide, diluted in 0.1 M phosphate buffer, pH 7.3 (Adams 1981), counterstained lightly with either cresyl violet or neutral red, and coverslipped with Permount. A second set of sections was processed for HRP histochemistry by incubation for 30 min in a solution of 0.025% 4-chloro-1-naphthol and 0.005% hydrogen peroxide diluted in Tris buffer (pH 7.6). A third set was processed for HRP histochemistry with 4-chloro-1-naphthol as chromogen (as above), rinsed well in Tris buffer, and subsequently processed for GAD immunocytochemistry with a rat GAD antiserum raised in sheep (Oertel et al. 1981a) by the double cycle PAP procedure as previously described (Nelson et al. 1989). Briefly, the sections were: (1) blocked for 1 h in 5% rabbit serum, (2) incubated at 4° C for three days in GAD antiserum (1:2000) with 1% rabbit serum, (3) incubated for 1 h in rabbit anti-sheep (1:50) with 1% rabbit serum, and then, (4) in goat PAP (1:100) with 1% rabbit serum. Steps 3 and 4 were repeated to amplify the reaction, and finally the sections were reacted in 0.05% DAB and 0.001% hydrogen peroxide. Tris buffer (0.5 M, pH 7.6) was used throughout as diluent and as rinsing solution after each step of the immunoreaction. The second and third sets of sections were wet-mounted in glycerol-phosphate buffer (1:3). Since 4-chloro-1-naphthol produces a blue reaction product, and DAB produces a brown reaction product, cerebellar neurons which contain retrogradely transported WGA-HRP and endogenous GAD were labeled with blue granules and a diffuse brown cytoplasm. Double-labeled neurons positive for both GAD and HRP and single-labeled neurons (either GAD-positive or HRP-positive) were mapped with the drawing tube of a light microscope.

In one rat receiving an injection of WGA-HRP into the IO, adjacent cerebellar sections were processed for HRP-histochemistry and counterstained with a Nissl method, or subjected to the double-labeling procedure for HRP and GAD detection described above, to determine the numbers and sizes of HRP-positive, GAD-positive, and double-labeled neurons. In Nissl-stained sections, neurons containing visible nucleoli were counted and categorized as HRP-negative or -positive. Their sizes were determined by measuring the longest soma diameter (so called 'long diameter') and the longest diameter normal to this (so called 'short diameter'). The product of the long and short diameters was used as an estimate of somatal 'area'. Adjacent sections processed by the double-labeling method were searched for the presence of GAD-positive or HRP-positive single-labeled neurons, and double-labeled neurons. These were counted if they contained a visible nucleus, and their somatal areas were determined, as described above. No correction formulas for split nuclei or nucleoli were used, since the values measured represent relative estimates.

Lesion-induced depletion of GAD. Since it is well known that severance of GABAergic axons results in a reduction of GAD immunostaining in their target regions (Ribak et al. 1980; Oertel et al.

1981c, 1983), we placed lesions in either of two different brain locations to destroy the cerebello-olivary projection. The cell bodies of the deep nuclei were removed by aspiration on both sides of the cerebellum in 4 rats, and on only one side in 13 rats. Another 10 rats received a coronally oriented knife cut on one side of the midbrain at the level of the inferior colliculus (Fig. 8), to transect the superior cerebellar peduncle, which contains the cerebello-olivary fibers (Achenbach and Goodman 1968; Graybiel et al. 1973). This lesion spares the climbing fibers, that reach the cerebellum via the inferior cerebellar peduncle. In a control group of three rats, large regions of the cerebellar cortex were aspirated without apparent damage to the underlying nuclei. Survival times between 4 and 63 days were tested, but we illustrate here only cases with survivals of 10 and 15 days, since these were optimal.

All operated rats were perfused transcardially with 200 ml of physiologic saline followed by 1000 ml of 0.5% zinc salicylate, 4% formaldehyde and 0.9% NaCl, pH 4.5, at room temperature. The brains were removed 1 h after perfusion, cryoprotected in saline containing 30% sucrose, and cut at 20 μm on a freezing microtome. Brains with cerebellar lesions were sectioned coronally through the brainstem and cerebellum. Brains with mesencephalic lesions were separated into two parts by a coronal cut through the medullary-pontine transition. The medulla was sectioned coronally, and the remaining brainstem was sectioned sagittally. Sections through the IO were processed for GAD immunocytochemistry as described above, and wet-mounted in a glycerol-phosphate buffer medium. The distribution of GAD-immunostained puncta in the IO were mapped with a microscope drawing tube, and compared with the distribution in nine normal unoperated rats from a previous study (Nelson and Mugnaini 1988). Sections containing the lesioned areas were Nissl-stained with cresyl violet, coverslipped with Permount, and the sites and extents of the lesions were mapped with a microscope drawing tube.

Electron microscopy (EM). EM-immunocytochemistry for GAD was performed according to previously described standard techniques (Oertel et al. 1981b; Adams and Mugnaini 1987), with some variations. Briefly, rats were perfused with a vascular rinse of Ringer solution saturated with 95% O_2 and 5% CO_2 to pH 7.2, followed by a fixative consisting of 4% paraformaldehyde and 0.1% glutaraldehyde in 0.12 M phosphate buffer, pH 7.3, and then by a second fixative of 4% paraformaldehyde in 0.12 M phosphate buffer. Vibratome sections were cut at 20 μm through the IO, and immunoreacted according to the procedure described above except that 0.1 M Tris-buffered saline (TBS) was used in place of 0.5 M Tris, and 0.0001% hydrogen peroxide was used in the DAB reaction step. Immunostained sections were postfixed with osmium, contrasted with uranyl acetate, dehydrated, and embedded by standard EM methods.

Anterogradely labeled cerebellar axons in the IO were analyzed by EM in two rats which had received injections of 5% WGA-HRP into the cerebellar nuclei. After a 3-day survival period, the rats were perfused with a Ringer solution followed by a fixative consisting of 0.5% paraformaldehyde and 2.5% glutaraldehyde, in 0.12 M phosphate buffer. The brains were Vibratome sectioned and processed for HRP with the TMB method of Mesulam (1978). The TMB reaction product was stabilized in 0.05% DAB, 0.025% cobalt hexachloride, and 0.02% nickel ammonium sulfate with 0.001% hydrogen peroxide in 0.2 M acetate buffer, pH 4.8. The sections were then osmicated, dehydrated and flat embedded. Ultrathin sections were prepared by standard procedures.

For anterograde degeneration study of the cerebello-olivary boutons, the superior cerebellar peduncle was transected by a knife cut. After either a 4- or 21-day survival period, the rats were perfusion-fixed with the protocol described above for EM-immunocytochemistry. The medulla was sectioned on a Vibratome at 100 μm and the slices were postfixed in ferricyanide-reduced osmium (2% osmium and 1.5% potassium ferricyanide in 0.1 M phosphate buffer), dehydrated, embedded, and thin-sectioned by standard procedures.

Results

WGA-HRP retrograde labeling of cerebellar and vestibular neurons projecting to the IO

The criteria for localizing cerebellar and vestibular neurons, labeled retrogradely from the territory of the IO, were based on the parcellation of the cerebellar nuclei provided by Ohkawa (1957) and Korenliussen (1968), and on the description of the vestibular nuclear complex by Mehler and Rubertone (1985). Large numbers of neurons in the lateral, the anterior interposed and the posterior interposed cerebellar nuclei, and small numbers of neurons in the ventrolateral region of the medial cerebellar nucleus and in the dorsal part of the lateral vestibular nucleus were retrogradely labeled by WGA-HRP injections restricted to the IO (Figs. 1 and 2). The product of the long and short diameters of the labeled neurons was less than 270 μm^2, with the majority measuring about 150 μm^2, and, therefore, these were categorized as 'small' neurons. Most of the labeled neurons were located contralateral to the injection site, and only a few were observed on the ipsilateral side (Figs. 1A, 2A, B). Larger neurons (somatal areas ranging from 270–750 μm^2) make up more than 50% of all nerve cells in the cerebellar nuclei; these were not retrogradely labeled when injections were restricted to the IO, but a few were labeled when tracer involved the reticular formation rostral to the IO (Fig. 2B).

When large tracer injections involved the caudal regions of the IO, retrogradely labeled cells were seen not only in the cerebellar and lateral vestibular nuclei, but also in the spinal vestibular, parasolitary, and ventral cuneate nuclei, and also in regions surrounding the hypoglossal nucleus and ventral to the cuneate nucleus. A subsequent paper will describe these projections in detail, since the present report is restricted to a description of the projections from the deep cerebellar nuclei, including the dorsal part of the lateral vestibular nucleus.

The combined maps of two cases with large tracer injections, depicted in Fig. 1A and B, showed that all regions of the cerebellar nuclei contain retrogradely labeled neurons, with the exception of a large portion of the medial cerebellar nucleus. Smaller tracer injections, illustrated in Fig. 2A and B, revealed a topographic cerebello-olivary projection similar to that described previously (see Dietrichs and Walberg 1989 for review). The lateral cerebellar nucleus projects to the principal olive (PO) (Fig. 2B), and the anterior interposed nucleus projects to the ventral fold of the dorsal accessory olive (DAO) (Fig. 2A, B). Only injections involving the rostral lamella of the medial accessory olive (MAO) labeled neurons in the posterior interposed nucleus (Fig. 1A, B). Neurons in the dorsal lateral hump were labeled when tracer filled the rostral-most aspect of the MAO (Fig. 1A). Small neurons of the dorsal lateral vestibular and medial cerebellar nuclei were labeled by tracer injections into the caudal regions of the IO (Fig. 1A, B), and like the projections from the lateral and interposed

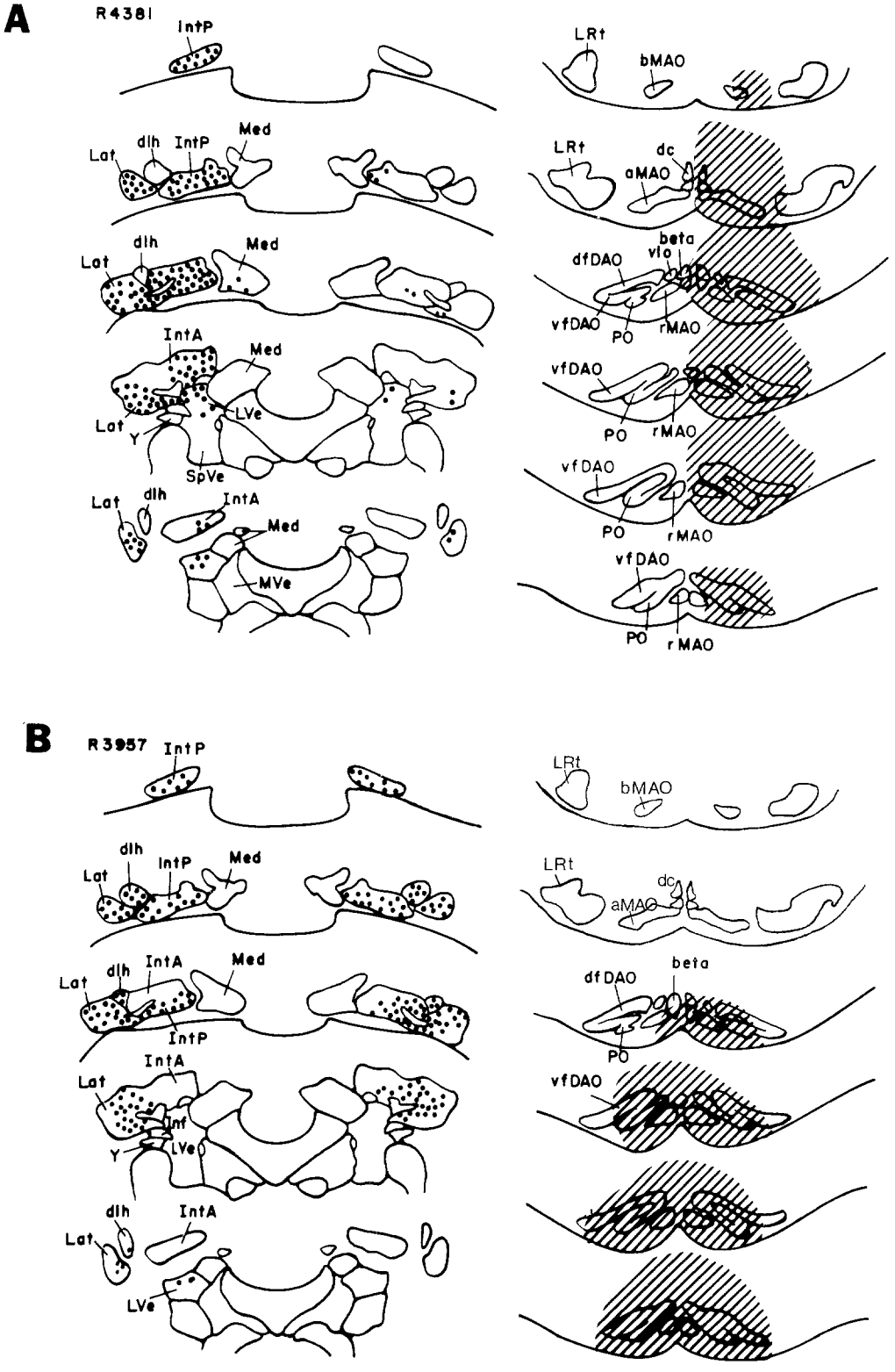

Fig. 1A, B. Maps showing the distribution of neurons retrogradely labeled (*dots*) in the cerebellar and vestibular nuclei after large tracer injections (*hatched areas*) into the IO.
A A large injection encompassing the IO on one side of the brainstem labels many neurons contralaterally in the lateral (*Lat*), the anterior (*IntA*), and posterior (*IntP*) interposed cerebellar nuclei, and in the dorsal part of the lateral vestibular nucleus (*LVe*). Fewer neurons are labeled ipsilaterally in these nuclei, and contralaterally in the medial cerebellar nucleus (*Med*).
B A bilateral injection involving all but the caudal third of the IO and the lateral parts of the rostral DAO labels neurons bilaterally in the dorsal lateral hump, the posterior interposed and lateral cerebellar nuclei, as well as a few neurons in the lateral cerebellar nucleus. Considered together, **A** and **B** demonstrate a finer topography, since neurons are labeled in the dorsal lateral hump only when the rostral MAO is included in the injection (labeled in **B** but not in **A**), and neurons are labeled in the anterior interposed nucleus only when tracer is placed in the lateral portion of the ventral fold of DAO (labeled in **A** but not in **B**)

cerebellar nuclei, these were also predominantly crossed. Thus, our results were in line with previous investigations of the topographic organization of the cerebello- and vestibulo-olivary projections in rat (Angaut and Cicirata 1982; Haroian 1982; Billard et al. 1989).

GAD immunocytochemistry combined with WGA-HRP tract-tracing

Our GAD immunostaining study confirmed previous reports of numerous GABAergic neurons in all of the cere-

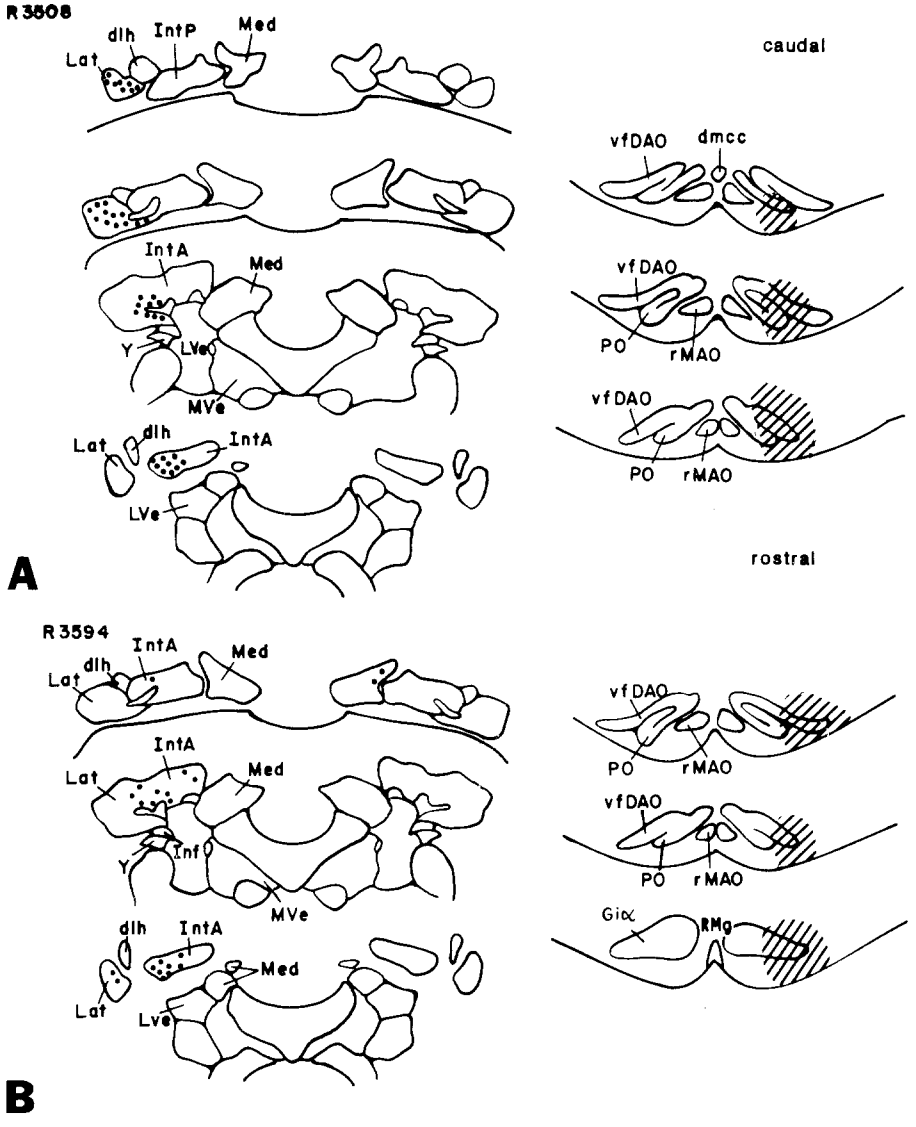

Fig. 2A, B. Distribution of neurons (*dots*) in restricted regions of the cerebellar nuclei retrogradely labeled after small tracer injections (*hatched areas*) into the IO.
A An injection of WGA-HRP involving the rostro-lateral part of the PO and the rostral part of the DAO labels neurons in the caudal aspect of the lateral cerebellar nucleus and the lateral part of the anterior interposed nucleus.
B A tracer injection involving the lateral part of the rostral DAO, a small part of the PO, and the gigantocellular reticular nucleus (*Gi α*) labels many small neurons in the anterior interposed nucleus, but only a few neurons in the lateral cerebellar nucleus. A few large neurons are also labeled in the ipsilateral medial cerebellar nucleus; this only occurs when the tracer spreads outside of the IO

bellar and vestibular nuclei (Chan-Palay et al. 1979; Mugnaini and Oertel 1981, 1985; Chan-Palay 1982; Houser et al. 1984) (Fig. 3). These neurons have previously been described as being immunostained with a moderate intensity, and best observed at low magnification with colchicine pretreatment (Oertel et al. 1981b). Although colchicine pretreatment was not used in the present study, the neurons appeared well stained by the protocol used, particularly when viewed at high magnification. The GABAergic neurons in the cerebellar nuclei and in the dorsal part of the lateral vestibular nucleus have a somatal 'area' of 270 μm^2 or less, and belong, therefore, to the small cell category. Larger (somatal 'area' larger than 270 μm^2) GAD-positive neurons of various sizes were present in other subdivisions of the vestibular nuclear complex, but these are beyond the scope of the present paper.

In order to test if the small GABAergic neurons of the cerebellar and lateral vestibular nuclei project to the IO, a double-labeling procedure was employed. Cerebellar sections of WGA-HRP injected rats were processed first by WGA-HRP histochemistry using 4-chloro-1-naphthol as the chromogen, and then by GAD immunocytochemistry with diaminobenzidine (DAB) as the chromogen. Projection neurons containing retrograded transported WGA-HRP were detected by the blue, granular reaction product in their cytoplasm (Fig. 4A). GABAergic neurons were labeled with a diffuse brown cytoplasm. GABAergic projection neurons (double-labeled neurons) contained both markers (blue granules in a diffuse brown cytoplasm) (Fig. 4B–D).

When injections of tracer were restricted to the IO territory, this double-labeling procedure revealed a substantial number of GABAergic projection neurons in all parts of the lateral and interposed cerebellar nuclei, the ventrolateral regions of the medial cerebellar nucleus, and the dorsal aspect of the lateral vestibular nucleus (Fig. 4B–D). The distribution of double-labeled neurons corresponded exactly to the distribution of cerebello-olivary neurons detected by WGA-HRP-histochemistry.

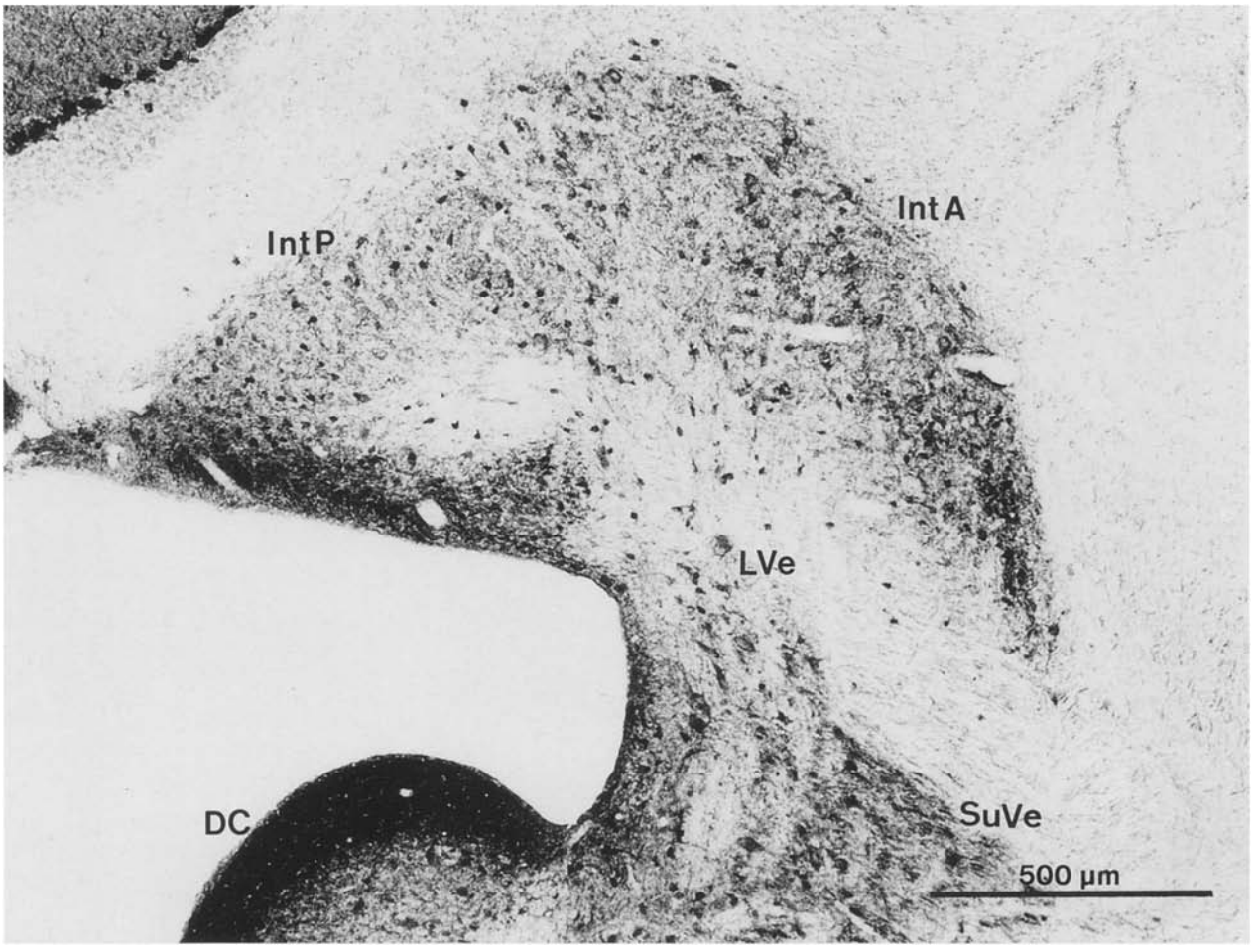

Fig. 3. Sagittal view of the cerebellar and vestibular nuclei. The anterior and posterior interposed cerebellar nuclei contain many small GAD-positive neurons. Fewer GAD-positive neurons are present in the dorsal region of the lateral vestibular nucleus (*LVe*). The superior vestibular nucleus (*SuVe*) contains larger immunostained neurons. All of these nuclei also contain GABAergic boutons, some of which delineate large GAD-negative somata in the cerebellar nuclei and the lateral vestibular nucleus

Furthermore, WGA-HRP-positive and GAD-negative single-labeled neurons were either absent, or, in a few cases, comprised only a small percentage of the total population of WGA-HRP-positive neurons. Conversely, in regions of the cerebellar nuclei which contained double-labeled neurons, nearly all of the GABAergic neurons also contained WGA-HRP. In all cases, no large neurons were GAD-positive.

These observations are illustrated quantitatively in Fig. 5. The histograms shown were obtained from a representative case, where a WGA-HRP injection was centered in the ventral fold of the DAO, thus labeling neurons in the anterior interposed nucleus. Nissl staining with neutral red shows that the somatal 'areas' range from 50 to 750 μm^2, but these fall into two groups: one group with areas between 50 and 270 μm^2, and another group of larger neurons with areas between 270 and 750 μm^2. Only neurons with somatal areas less than 270 μm^2 were HRP-positive. In one section, 46.5% of

Fig. 4 A–D. Double-labeled neurons. Combining WGA-HRP histochemistry with GAD immunocytochemistry reveals the presence of small GABAergic projection neurons in the cerebellar and lateral vestibular nuclei. **A** Section processed by HRP histochemistry using 4-chloro-1-naphtol as chromogen. The cytoplasm of a small neuron (*solid arrow*) in the lateral cerebellar nucleus contains blue granular reaction product of HRP retrogradely transported from the IO. *Open arrow* points to the nucleolus of a large unlabeled neuron, and *n* indicates neuronal nuclei. **B** Section processed by HRP histochemistry and GAD immunocytochemistry. Two small neurons in the lateral cerebellar nucleus contain WGA-HRP (blue granules) and GAD (diffuse brown cytoplasm), and are, therefore, GABAergic projection neurons. **C** A small double-labeled neuron (*arrow*) and four large unlabeled neurons (*asterisks*) outlined by GABAergic boutons in the lateral cerebellar nucleus. *Open arrow* points to the nucleolus of a large unlabeled neuron. The surrounding neuropil also contains many GAD-positive boutons, some of which surround dendritic profiles. **D** Two small GAD-positive neurons (*arrows*) lightly labeled with HRP granules, and three large unlabeled neurons (*asterisks*) delineated by GABAergic boutons in the dorsal part of the lateral vestibular nucleus

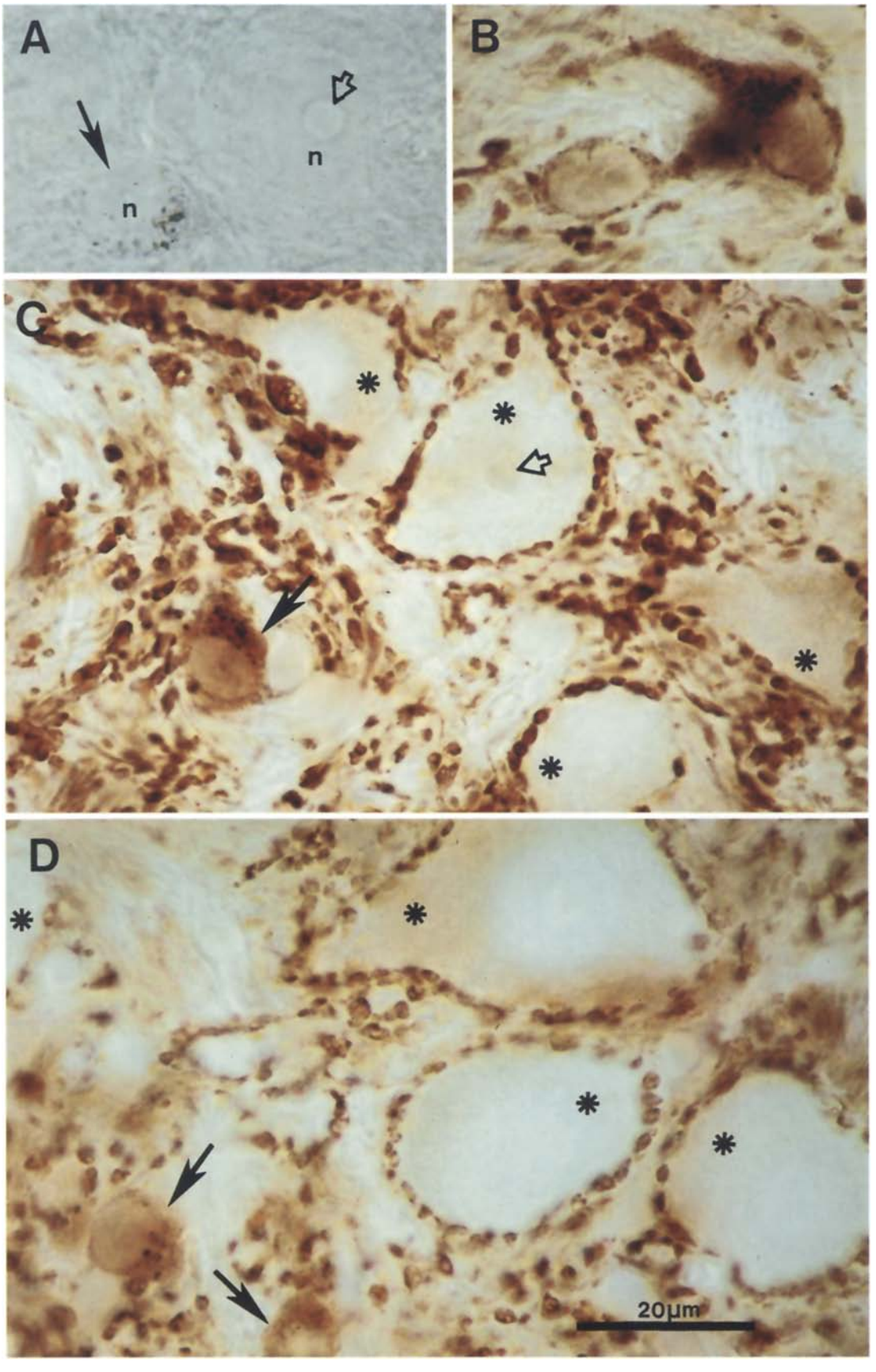
A
n
n
B
C
D
20µm

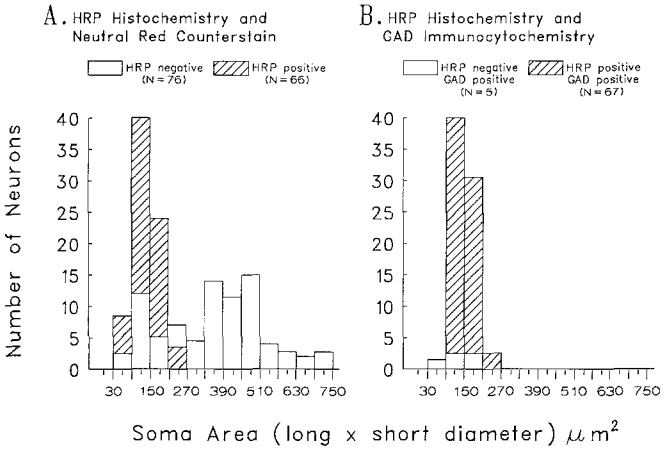

Fig. 5A, B. Histograms of neuron sizes in the anterior interposed nucleus from a rat with a tracer injection centered in the ventral fold of the DAO. **A** From a cerebellar section processed by HRP histochemistry (DAB-heavy metal intensification method, Adams 1981) and counterstained with neutral red. WGA-HRP-positive neurons (*striped bars*) all have somatal areas of 270 μm² or less, while the WGA-HRP-negative neurons (*open bars*) have areas as large as 750 μm². **B** An adjacent cerebellar section processed by the double-labeling protocol. All GAD-positive neurons have small somatal areas of 270 μm² or less, and nearly all of these are also WGA-HRP-positive (*striped bars*). No neurons that appeared WGA-HRP-positive but GAD-negative were observed in this rat

the total neuronal population (66 neurons) was WGA-HRP-positive, but about 72% of the small neurons were retrogradely labeled (Fig. 5A). WGA-HRP-histochemistry and GAD immunocytochemistry of an adjacent section labeled 72 neurons as GAD-positive, all of which were smaller than 270 μm². Of these, 93.1% (67 neurons) were also WGA-HRP-positive (Fig. 5B). Thus, in this experiment, a large portion of the small neurons in the anterior interposed nucleus projected to the IO, and all of the projection neurons had small, GAD-positive cell bodies. Also, only 6.9% of the GABAergic neurons were not tracer-labeled in this experiment, demonstrating that, at most, only a minor population of GABAergic neurons does not project to the IO.

Lesion-induced depletion of GABAergic boutons

GAD immunocytochemistry of the rat IO shows nonhomogeneities in the density and the size of GABAergic boutons that can be matched to the projection areas of certain afferent systems (Nelson and Mugnaini 1989; Nelson et al. 1989). A large portion of the rat IO contains relatively small GABAergic boutons that produce an intermediate GAD immunostaining intensity. If these boutons are supplied in large part by a single afferent source, then the destruction of this source should result in degeneration of the axons, and a subsequent depletion of GABAergic boutons in the target regions. This procedure was chosen as a means of verifying the extent of the contribution of the cerebello-olivary projection to the GABAergic innervation of the IO, and to map the target boundaries of this projection.

Lesions of the cerebellar nuclei produced an extreme paucity of GAD-positive boutons in large regions of the IO as compared to normal rats (Figs. 6A, B and 7). A reduction from normal was first observed 4 days after the cerebellar lesion, and was maximal 10 days after the lesion. Only scattered GAD-positive boutons remained in the entire PO, the rostral lamella of the MAO, the ventrolateral outgrowth, and ventrolateral portions of the ventral fold of the DAO. These effects occurred bilaterally in totally cerebellectomized rats, and contralaterally in hemicerebellectomized rats. Lesions that involved the dorsal aspect of the lateral vestibular nucleus as well as the cerebellar nuclei produced a striking loss of GABAergic boutons also in the contralateral dorsal fold of the DAO (Fig. 9C). None of the operated animals included in this study had any visually detectable loss of GABAergic boutons in the beta nucleus, the dorsal cap, the subnuclei a, b or c of the MAO, the dorsomedial cell column, or a dorsomedially located strip of the ventral fold of the DAO. Also, GAD-positive boutons remained along the ventral border of the rostral MAO and in the rostral-most tip of the MAO, although some depletion was observed in these regions.

Lesions of the cerebellum eliminate cerebello-olivary neurons, but they also destroy the axons of the inferior olivary neurons, which terminate in the cerebellar nuclei as branching fibers, and in the cerebellar cortex as climbing fibers (Desclin 1974; Wiklund et al. 1982; Mugnaini and Nelson 1989; Cummings et al. 1989). After cerebellectomy, therefore, a loss of GABAergic innervation in the IO might result from the retraction of GABAergic boutons consequent to a retrograde effect on axotomized olivary neurons, as demonstrated in motoneurons (Chen 1978). If this were the case, however, one would have to explain why some regions of the IO appear normal after cerebellectomy, in spite of the complete or near complete severance of the olivocerebellar axons. Anyway, the above possibility can be excluded by lesion of the axons of the cerebello-olivary projection without damage to the cerebellum. These axons from part of the superior cerebellar peduncle as they course rostrad to the level of the red nucleus, decussate, and project ventrocaudally to the brainstem (Achenbach and Goodman 1968). This pathway was therefore transected with a knife cut at the level of the inferior colliculus (Fig. 8). In most cases, the ascending bundle was partially transected on only one side of the brain, thus affecting a part of the projection to the contralateral IO. In other cases, the lesion of this bundle was total or subtotal, but also partially damaged the contralateral fibers. These lesions produced a loss of GABAergic boutons within the appropriate olivary regions and over the same time course as established by cerebellectomy (Figs. 6B, 8A), although no depletion was observed in the dorsal fold of the DAO. This latter point led us to speculate that the vestibulo-olivary fibers take a tegmental course, rather than projecting in the superior cerebellar peduncle. The results demonstrate that the post-cerebellectomy loss of GABAergic boutons in the IO is due to degeneration of cerebello-olivary fibers. Furthermore, removal of large regions of cerebellar cortex, with no apparent

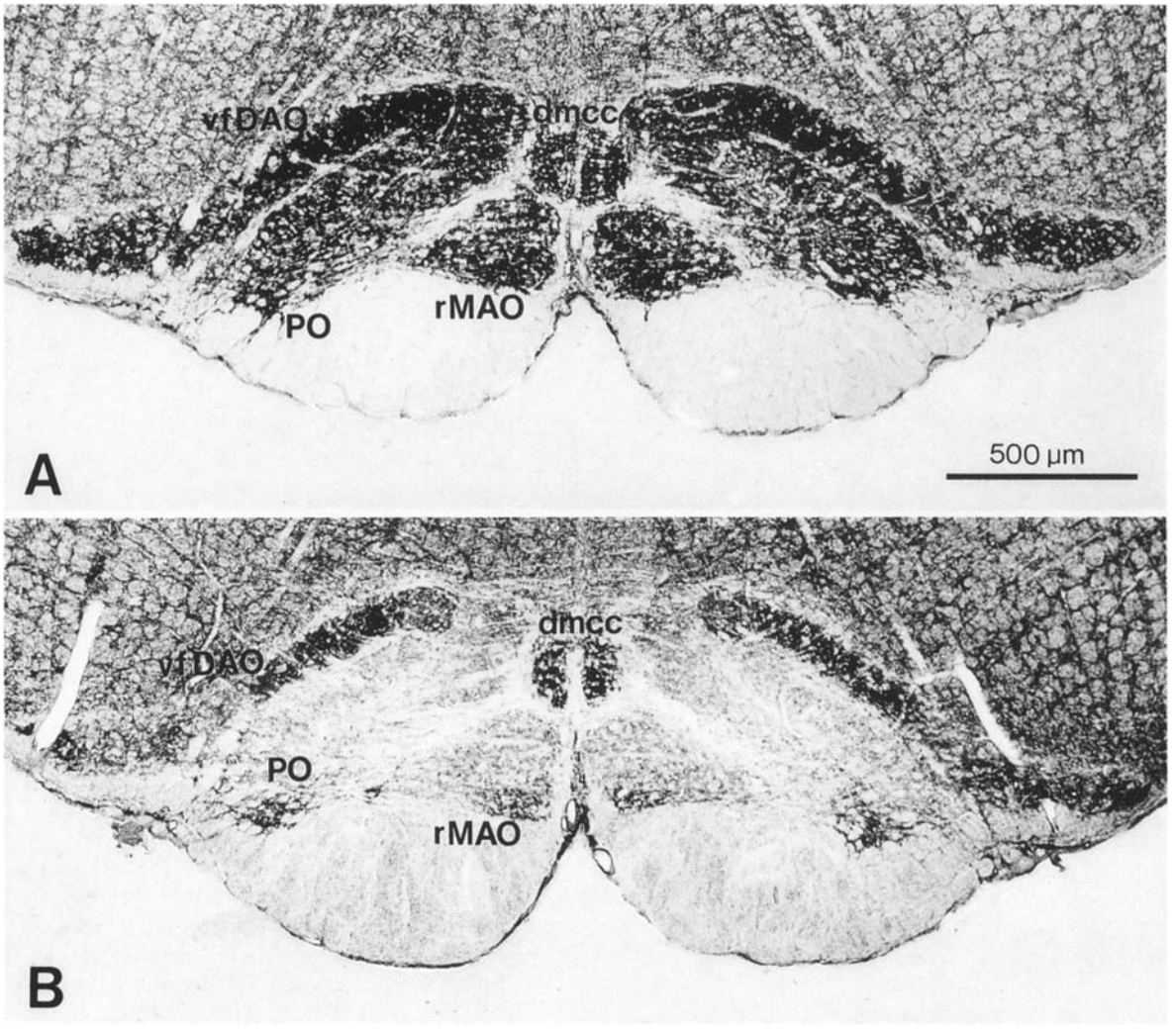

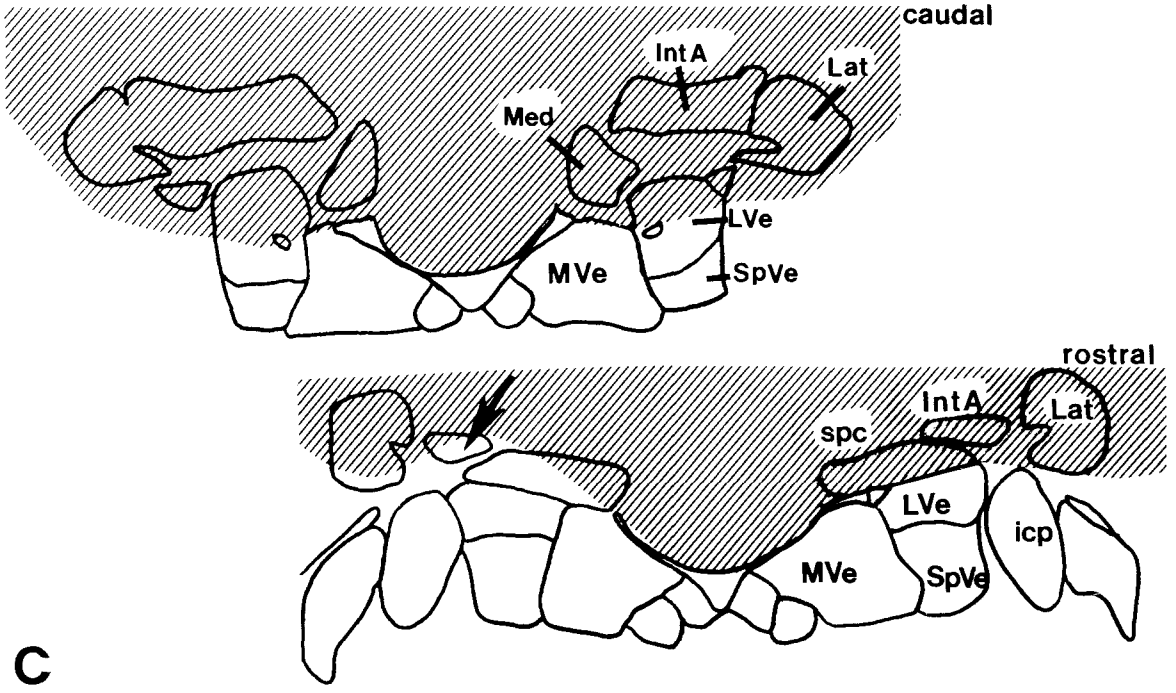

Fig. 6A–C. Depletion of GAD-positive boutons in the IO after lesion of the cerebellar nuclei. **A** GAD-positive boutons densely populate the neuropil of the IO in normal rat. **B** Within 10 days after a nearly total aspiration of the cerebellar nuclei, a striking depletion of GAD-positive boutons occurs in the PO, rostral lamella of the MAO, and the lateral part of the ventral fold of DAO. A high density of GAD-positive boutons remains in the medial aspect of the DAO and the dorsomedial cell column. **C** Schematic representation of regions removed from the cerebellum (*hatched area*) to produce the depletion observed in the case illustrated in **B**. A rostral portion of the left anterior interposed nucleus remains (*arrow*), which probably accounts for the failure to deplete GAD-positive boutons in the right lateral portion of the DAO

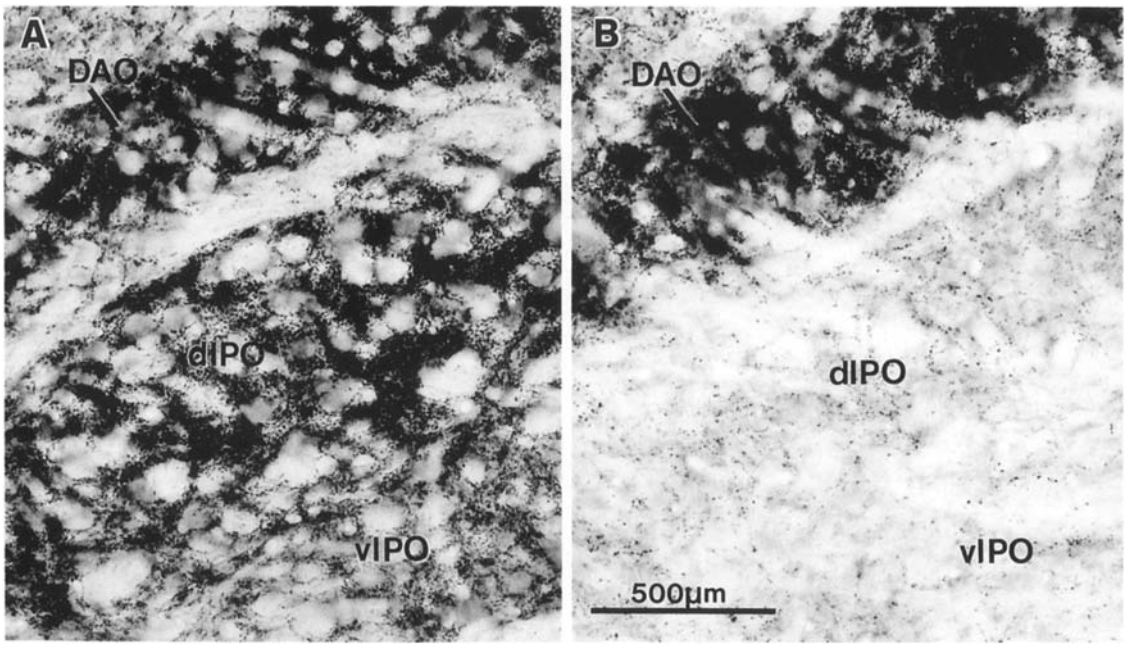

Fig. 7A, B. Lesion-induced depletion of GAD immunostaining in the IO observed at higher magnification. PO (dorsal and ventral lamella) and DAO of a normal rat (**A**) and a rat with lesion of the cerebellar nuclei (**B**). Only sparse GAD-positive boutons are present in the PO of the cerebellar lesioned rat, while staining appears normal in the medial part of the DAO

damage to the underlying nuclei, produced no observable depletion of GAD-positive boutons in the IO within 15 days. A map of olivary regions affected by lesions of the cerebellar and lateral vestibular nuclei is presented in Fig. 10.

The target regions of the cerebellar and the lateral vestibular projections in the IO were largely confirmed by anterograde WGA-HRP transport, although some differences were observed. Tracer injections involving the interposed and lateral cerebellar nuclei resulted in bouton labeling of the contralateral IO in all of the striped regions in Fig. 10, and injections involving the lateral vestibular nucleus produced anterograde labeling in the contralateral dorsal fold of the DAO, which are the olivary regions depleted of GAD after cerebellar or lateral vestibular lesions. However, anterograde labeling was also observed in the intensely GABAergic region of the ventral fold of DAO, and in the rostral tip of the MAO, two regions that were not depleted of GABAergic boutons after cerebellar or superior cerebellar peduncle lesions. Another region not depleted of GABAergic boutons by any cerebellar lesion, the subnucleus b of MAO, contained anterogradely labeled boutons when tracer injections involved the medial cerebellar nucleus. One explanation is that these additional projections are not GABAergic, or alternatively, that they are GABAergic, but are minor, and overlap with other non-cerebellar GABAergic inputs in the IO, so that their removal does not produce a visible depletion of immunostained boutons.

Electron microscopy of cerebello-olivary axons in the PO

Three approaches were used to examine the GABAergic cerebello-olivary projection, as originally reported (Nelson et al. 1984). First, the ultrastructural characteristics of GABAergic boutons in the PO were explored by GAD-immunostaining. Second, WGA-HRP anterogradely transported from the lateral cerebellar nucleus to the PO was used to label axons of the cerebello-olivary pathway. Third, lesion of the superior cerebellar peduncle was used to produce anterograde degenerative changes in the cerebellar axons within the PO. The characteristics of axonal profiles labeled by these three methods were compared and, in combination, were used to describe the relationship that the boutons of the cerebello-olivary neurons share with other cell profiles in the PO.

Axonal profiles immunopositive for GAD were observed within the astrocyte-enclosed glomeruli of the PO, although many were also observed synapsing on neuronal cell bodies and proximal dendrites. All glomeruli encountered contained GAD-positive boutons. Many of these boutons were observed synapsing on one or both dendrites which were joined by a gap junction, with the synapse being located in very close proximity to the gap junction (Fig. 11). The boutons contained pleomorphic vesicles and formed predominatly symmetrical synaptic junctions characteristic of inhibitory synapses (but see Sotelo et al. 1986). No GAD reaction product was observed in boutons containing rounded vesicles. WGA-HRP anterogradely transported from the lateral cerebellar nucleus also labeled axonal boutons containing pleomorphic vesicles, in contact with small dendritic profiles joined by gap junctions (Fig. 12A). When anterograde degeneration was used to label the cerebello-olivary axons, a flocculent type of degeneration was observed after 4 days (Fig. 12B). The affected boutons were enlarged and vesicles, absent from other areas of the bouton, were clustered near the synaptic junctions. As in the GAD-

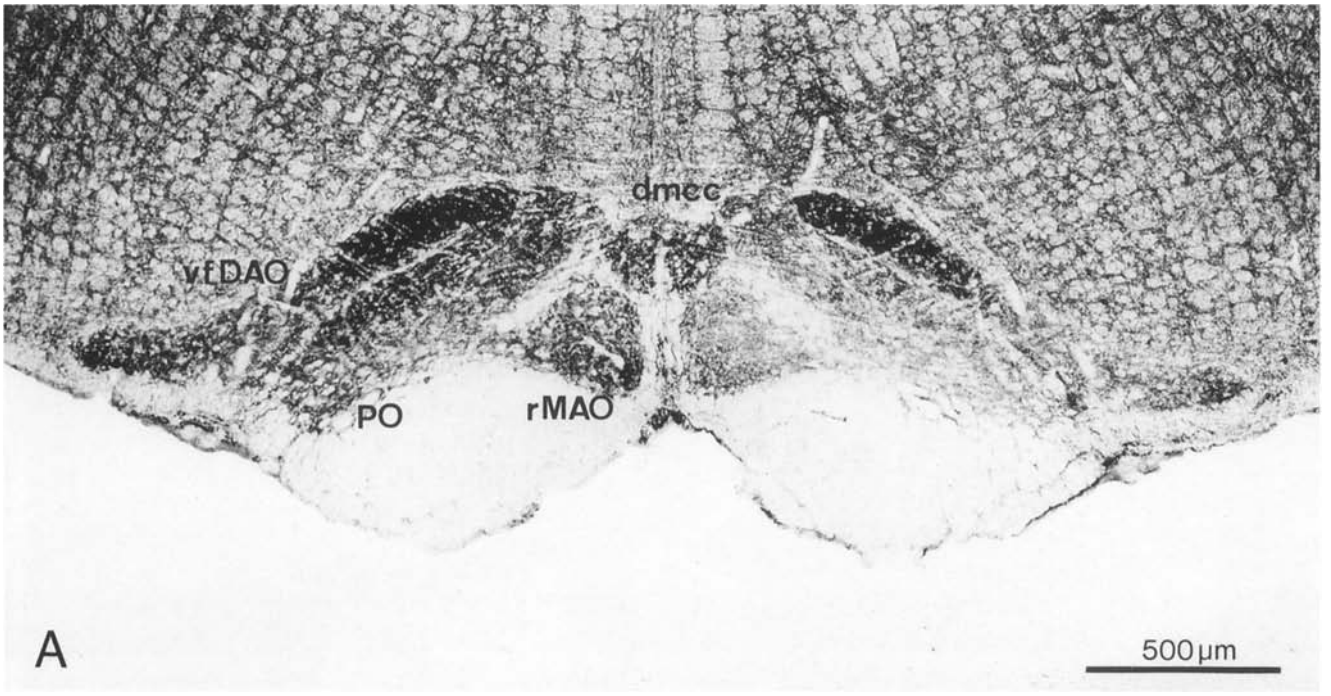

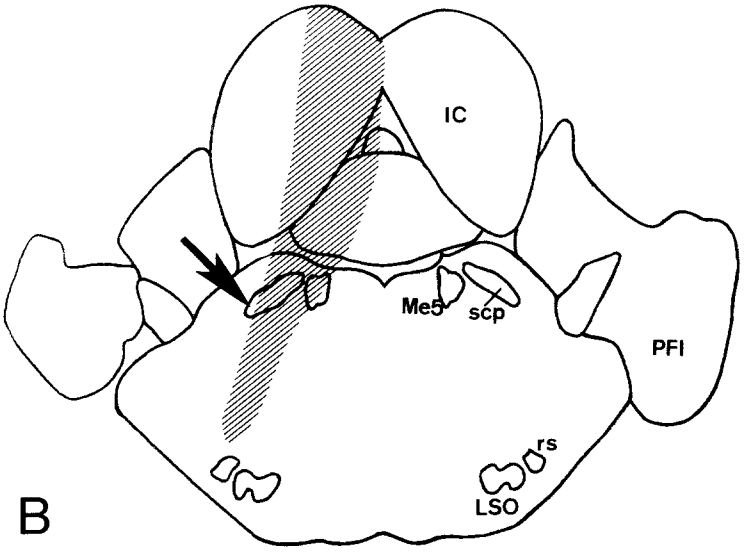

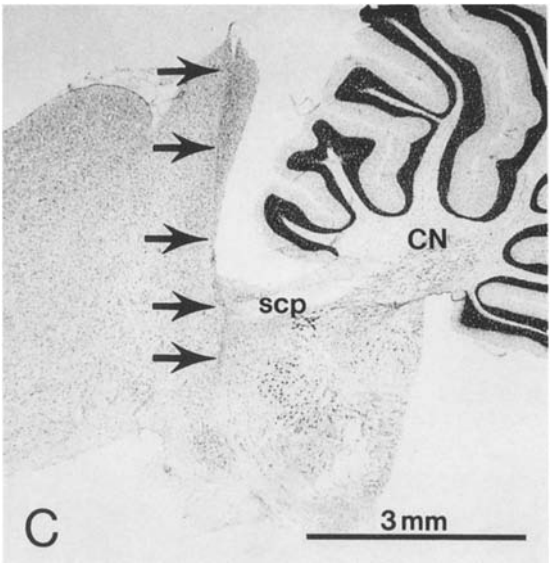

Fig. 8A–C. Depletion of GAD-positive boutons in the IO after transection of the superior cerebellar peduncle (*scp*). **A** A nearly complete transection of the left superior cerebellar peduncle produces a substantial depletion of GAD-positive boutons in the contralateral PO, the rostral lamella of the MAO, and the lateral part of the ventral fold of the DAO, that is, the same olivary regions affected by cerebellectomy. **B** Diagrammatic representation of the lesion site producing the depletion shown in **A**. In this case, all but the lateral portion of the superior cerebellar peduncle (*arrow*) was transected, which may have spared some GABAergic axons projecting to the contralateral IO. **C** Nissl-stained sagittal section of the brainstem and the cerebellum showing damage due to a knife cut (*arrows*) which severed the axons of the cerebello-olivary neurons in the superior cerebellar peduncle, but spared the olivo-cerebellar fibers, which course in the inferior cerebellar peduncle. *CN*, cerebellar nuclei

positive and the WGA-HRP labeled boutons, the vesicles of degenerating boutons were pleomorphic, and the boutons often formed axo-dendritic synapses near the gap junctions. No degenerative changes were observed in boutons containing rounded vesicles. Olivary glomeruli examined 21 days after transecting the superior cerebellar peduncle (Fig. 12C) rarely contained axonal boutons with pleomorphic vesicles, since by this time the cerebello-olivary axons had completely degenerated. This paucity of boutons with an 'inhibitory' morphology is consistent with the strong depletion of GAD-positive boutons observed at the LM level 10 days or more after lesion of the cerebellar nuclei or the superior cerebellar peduncle.

Discussion

The present study shows that the projection from the cerebellar nuclei to the inferior olive is massive and en-

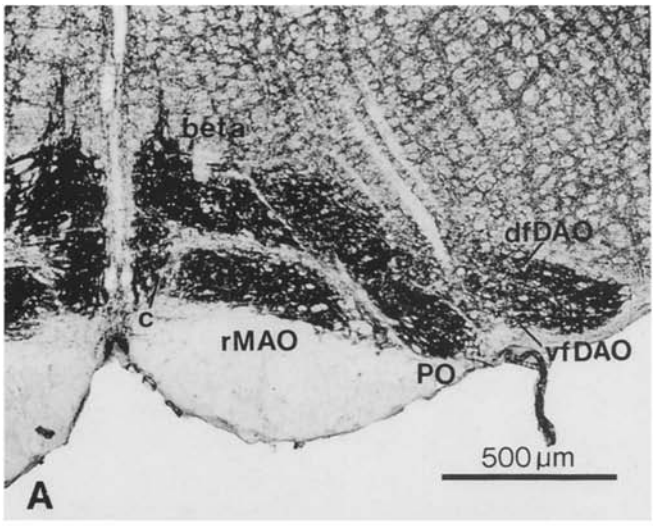

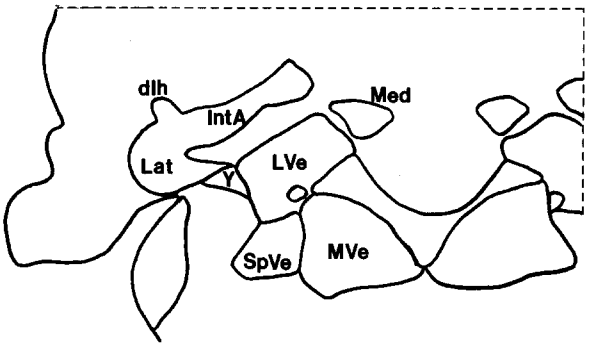

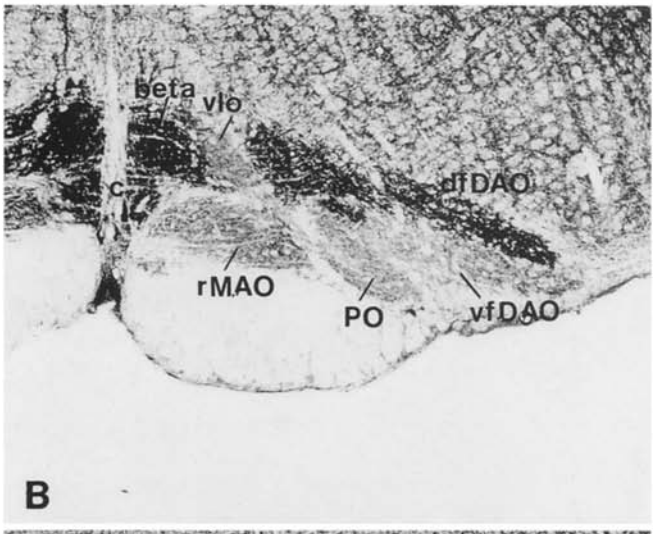

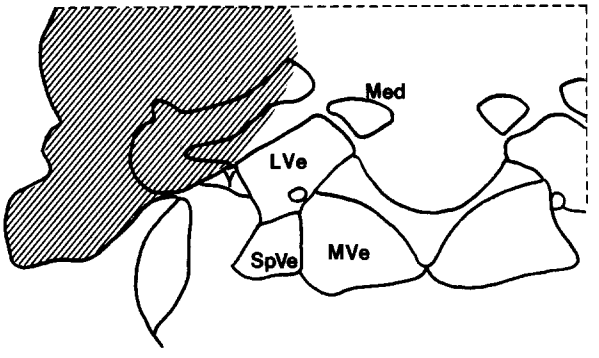

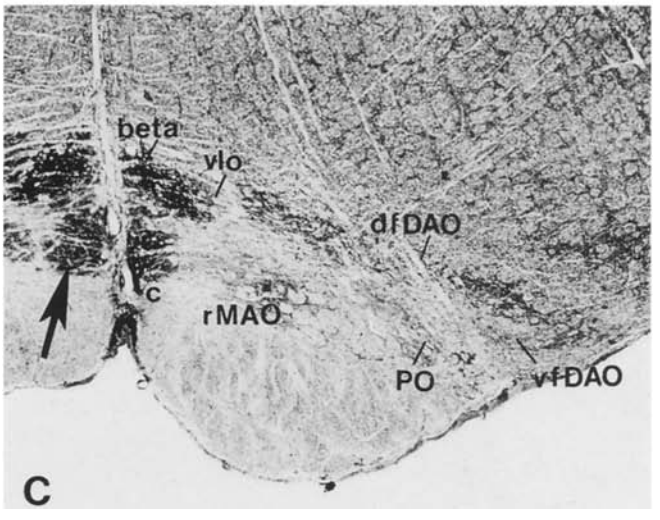

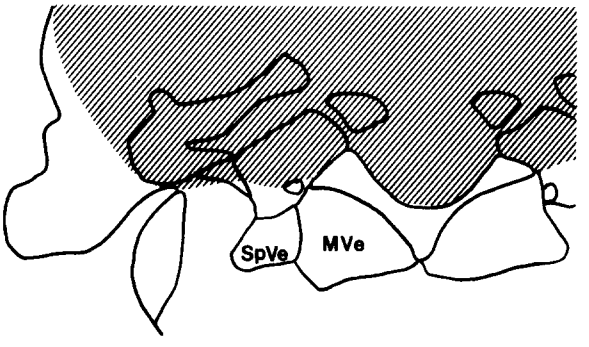

Fig. 9 A–C; A1–C1. Lesion-induced depletion of GABAergic boutons in the caudal aspect of the IO (**A–C**), and the corresponding maps of the lesion sites producing the depletion (**A1–C1**). **A** In a normal rat, all subnuclei of the IO contain a high density of GAD-positive boutons. **B** Removal of the cerebellar nuclei, shown schematically in **B1,** depletes GAD-positive boutons in the ventrolateral outgrowth, the rostral lamella of the MAO, the PO, and the ventral fold of the DAO. Immunostaining remains unchanged in the beta nucleus, subnucleus c of the MAO, and the dorsal fold of the DAO. **C** After a larger lesion to include the cerebellar nuclei and the dorsal part of the lateral vestibular nucleus (**C1**), few GAD-positive boutons remain in the dorsal fold of the DAO, as well as in the regions affected by destruction of the cerebello-olivary projection (ventrolateral outgrowth, rostral lamella of MAO, PO, ventral fold of DAO). This lesion also caused some damage to the parasolitary nucleus in the dorsal brainstem (not shown), which resulted in a reduction of GAD-positive boutons in the ipsilateral subnucleus c (*arrow*)

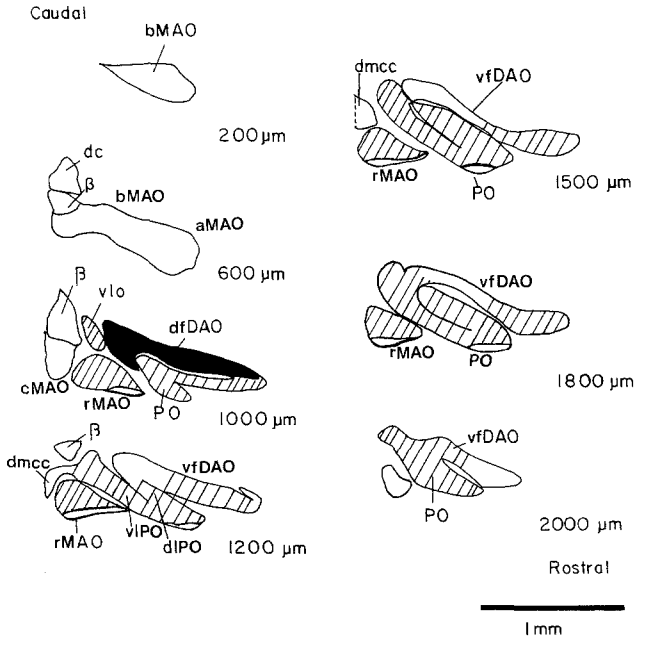

Fig. 10. Map of olivary regions depleted of GAD-positive boutons after a cerebellar lesion that extended into the lateral vestibular nucleus. Regions affected by cerebellectomy are shown by *hatching*. In *black* is the olivary region affected by destruction of the lateral vestibular nucleus. Although most of the inferior olive is affected by this lesion, some olivary regions appear distinctly normal (*white areas*), and must therefore receive their GABAergic input from other spared centers

tirely GABAergic, thus providing evidence that an important inhibitory projection originates from the cerebellar nuclei. These results were originally presented in lectures and also as preliminary reports (Nelson et al. 1984; Nelson and Mugnaini 1985, 1989), whose major points have successively been confirmed by other investigators (Sotelo et al. 1986; Angaut and Sotelo 1987; deZeeuw et al. 1988, 1989). Prior to this group of studies, all cerebellar output was thought to be excitatory (reviewed by Ito 1984), including the cerebello-olivary projection (Kitai et al. 1975; Chan-Palay 1977; King et al. 1976).

The inhibitory cerebello-olivary projection

Consistent with our observation that the cerebello-olivary projection is entirely GABAergic and, therefore presumably inhibitory, are reports by Andersson and Hesslow (1987a, b) that climbing fiber inhibition is correlated to increased activity of interposed nuclear neurons, and that stimulation of the superior cerebellar peduncle inhibits climbing fiber activity (Hesslow 1986). This inhibition of the IO is abolished by transection of the superior cerebellar peduncle (Andersson and Hesslow 1986). The presence of pleomorphic vesicles often associated with symmetrical synaptic junctions also suggests that the cerebello-olivary boutons are inhibitory (Peters et al. 1991).

Our observations and those of other investigators (Sotelo et al. 1986; Angaut and Sotelo 1987), particularly the recent detailed study of the cerebello-olivary projection in cat by deZeeuw et al. (1989, 1990a), demonstrate that this projection often provides synapses near gap junctions. Although in this study, we have not directly shown anterogradely labeled boutons to be GABAergic, taken together, our observations provide strong evidence that they belong to the GABAergic cerebello-olivary axons. Angaut and Sotelo (1987) have also described the synaptic relationship of anterogradely labeled cerebellar axonal boutons, presumed to be GABAergic, in the rat IO. Recently, experiments in the cat by deZeeuw et al. (1988, 1989) have directly demonstrated at the EM level that the cerebello-olivary projection is GABAergic, by double-labeling the boutons with GABA-immunogold and anterogradely transported WGA-HRP. In all of these experiments, cerebellar and/or GABAergic boutons synapsed near gap junctions. This observation strongly support the notion that GABAergic neurotransmission modulates the electrical coupling of olivary projection neurons (Llinás 1974, 1989). Llinás and coworkers (Sasaki and Llinás 1985; Llinás and Yarom 1986) have obtained evidence for this modulatory role of GABA, as they have observed an increase in the synchronization of harmaline-induced climbing fiber responses when GABA activity is blocked by picrotoxin application. DeZeeuw et al. (1990a, b) observed that the dendritic spines in each olivary glomerulus receive synapses from both non-GABAergic mesencephalic afferents and GABAergic cerebellar nuclei afferents. This suggests the attractive hypothesis that the organization of excitatory and inhibitory inputs to dendritic spines, provided by mesencephalic and cerebellar axons, respectively, serves to regulate the elecrical coupling and firing frequency of olivary neurons in a way that is extremely sensitive to the timing of these inputs (deZeeuw et al. 1990b). Whether cerebellar nucleo-olivary afferents synapsing on extraglomerular targets (i.e., dendritic stems, cell bodies and initial axon segments of olivary neurons), as observed by us in rat and by deZeeuw et al. (1989, 1990c) in the cat, produce other types of inhibitory effects remains to be demonstrated. Also, the precise mode of termination of cerebello-olivary fibers in the various olivary subnuclei still has to be analyzed.

Cytology of the cerebello-olivary neurons

The GABAergic cerebellar neurons projecting to the IO were less than 270 μm^2 in cell body area, and were thus classified as small cells. This is consistent with the findings of several cerebello-olivary projection studies (Tolbert et al. 1976, 1978; Brown et al. 1977; Legendre and Courville 1987). Some authors have described larger cerebellar neurons, usually located in the medial nucleus that project to the IO (Dietrichs and Walberg 1981; Swenson and Castro 1983a), but we have only observed such neurons when tracer injections involved the reticular nuclei, located dorsal and rostral to the IO, known to receive cerebellar afferents (Carrea and Mettler 1955; Cohen et al. 1958; Mehler et al. 1958; Carpenter and Nova 1950; Mehler 1967; Achenbach and Goodman 1968; Tolbert et al. 1980).

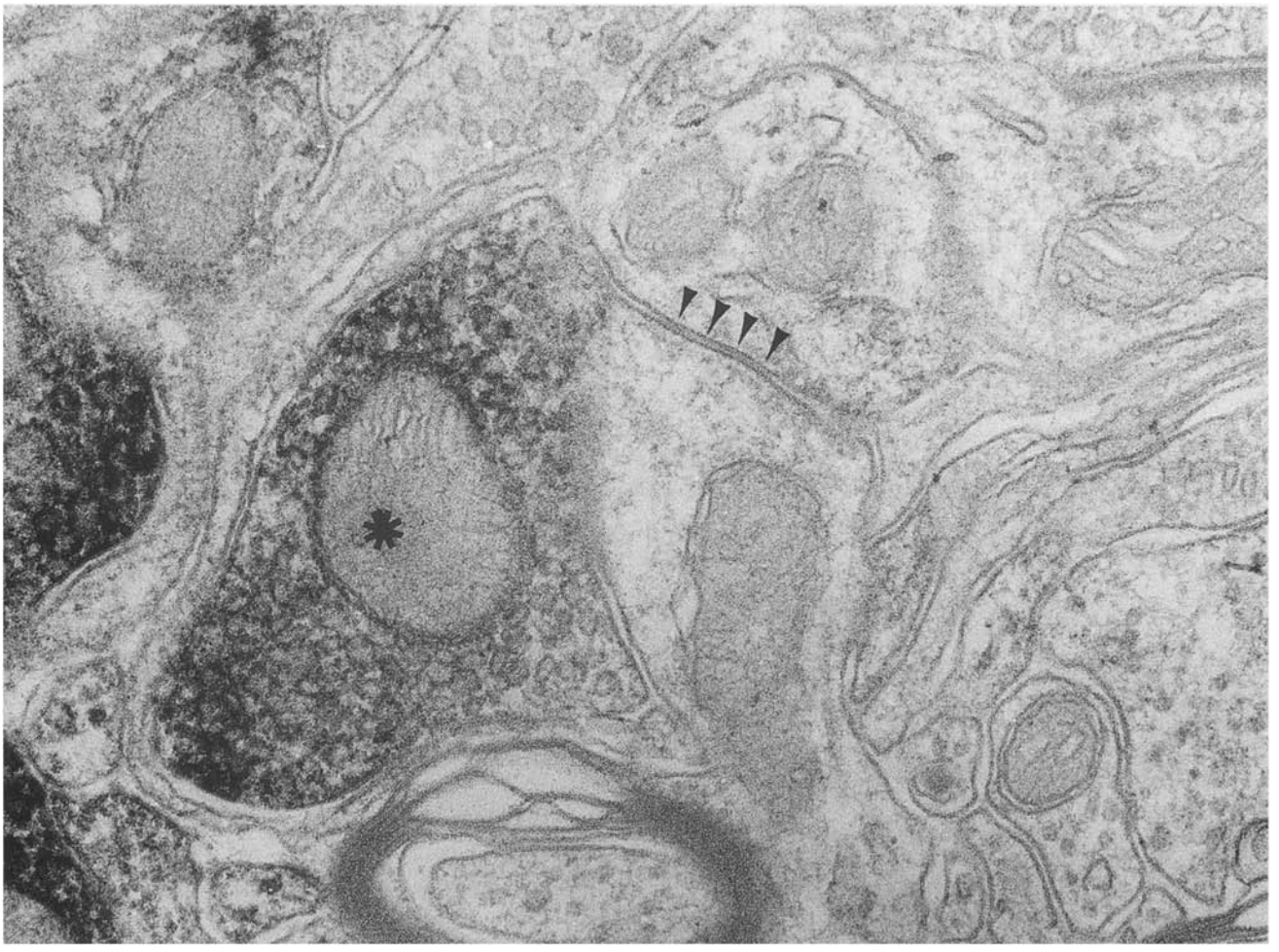

Fig. 11. Electron microscopy of GAD immunostaining in the PO. A GAD-immunostained bouton (*asterisk*) in a glomerulus of the PO contains pleomorphic vesicles, and contacts two dendric profiles joined by a gap junction (*arrowheads*). ×81200

A long-standing controversy as to whether the cerebellar nuclei contain interneurons currently remains unresolved. Early Golgi studies of Saccozzi and Lugaro (cited in Ramon y Cajal 1911) describe the presence of short axon neurons in the human dentate nuclei, but Ramon y Cajal (1911) did not observe any such neurons in the many mammalian species he investigated. In later Golgi studies (Matsushita and Iwahori 1971; Chan-Palay 1977) axonal branches of small neurons were observed to terminate within the cerebellar nuclei, but these studies do not exclude the possibility that they are branches of axons which also project out of the cerebellum. Flood and Jansen (1966) were able to produce degenerative changes in nearly all of the neurons of each cerebellar nucleus by transecting the cerebellar peduncles. McCrea et al. (1978) have labeled the vast majority (93%) of the neurons in the interposed cerebellar nuclei by HRP injections into known target regions, leaving only a small percentage of interposed nuclei neurons as possible local circuit neurons. Small GABAergic neu-

Fig. 12A–C. Electron microscopy of cerebello-olivary axons in glomeruli of the PO. **A** Two axonal profiles labeled by HRP-TMB reaction product present in the PO after injection of WGA-HRP into the lateral cerebellar nucleus. One of these boutons (*asterisk*) synapses on two dendritic spines joined by a gap junction (*arrowheads*). The labeled boutons contain pleomorphic vesicles, but no labeling is observed in the nearby boutons containing rounded vesicles (*star*). **B** Degenerating axonal bouton (*asterisk*) synapses with two dendrites and a spine 4 days after transection of the superior cerebellar peduncle. In the cerebello-olivary axons, early degeneration is characterized by swelling of the bouton, flocculent axoplasm, clumping of the vesicles near synaptic sites (*arrows*) and appearance of glycogen granules. No degeneration is apparent in nearby boutons containing rounded vesicles (*stars*). Like the GAD-positive and the WGA-HRP-labeled boutons, the degenerating boutons contain pleomorphic vesicles. **C** In portion of the olivary neuropil 21 days after transection of the superior cerebellar peduncle, degenerated cerebello-olivary axons have been eliminated from the PO, and only boutons containing rounded vesicles can be observed (*stars*). One of these boutons synapses near a gap junction joining two dendrites (*arrow*). **A, B** ×38100; **C** ×30800

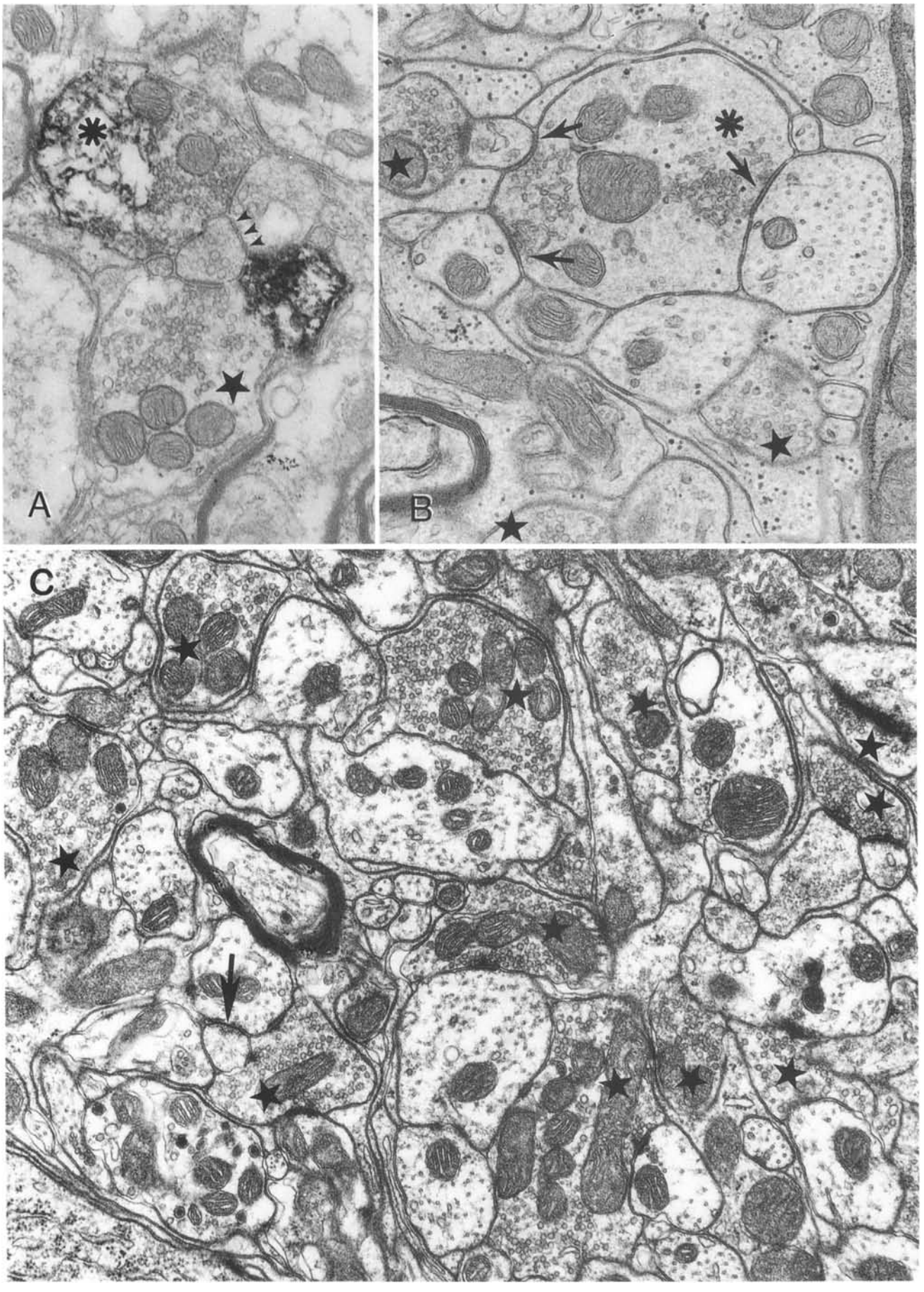
A
B
C

rons in the dentate nucleus were suggested to be inhibitory interneurons by Chan-Palay (1977, 1979), but Tolbert has argued that such cells may also be projection neurons (Tolbert and Bantli 1980; Tolbert 1982). In the present study, we have observed that when tracer injections were centered in specific olivary regions, nearly all of the GABAergic neurons in the corresponding cerebellar region were HRP labeled, thus indicating that the vast majority of GABAergic neurons in the cerebellar nuclei project to the IO. In one case, 93% of GABAergic neurons in the anterior interposed nucleus were also labeled by HRP retrogradely transported from the DAO. The small percentage of GABAergic neurons that were not retrogradely labeled by tracer could represent a population which does not project to the IO, or could be projection neurons that were not successfully labeled by the tracer.

In most rats, small GAD-negative neurons retrogradely labeled by HRP were absent when tracer injections were restricted to the IO, and in the few cases where they were observed, they comprised only a few percent of the total number of HRP-labeled neurons. These few neurons, however, could represent false negative data, due to a failure to stain them by the immunocytochemical method. Cells cut open during sectioning and exposed to the surface of the section are easily penetrated by the immunoreagents, but some cells embedded entirely within the section may fail to become immunostained even if they contain the antigen. This possibility cannot be excluded in our material, since the thickness of the sections was sometimes greater than the longest diameters of many cells. Immunoreagents, especially the large PAP complex, do not penetrate more than a few microns into the section without detergent treatment, and this may have prevented staining of the deeply embedded neurons. Detergent treatment cannot be used to demonstrate small GAD-positive neurons, since it leads to a staining of GAD-positive terminals only (Mugnaini and Oertel 1985). The occurrence of WGA-HRP-positive GAD-negative small neurons was inconsistent, and this supports a methodological explanation for such neurons, although the existence of a population of small GAD-negative neurons which do not project to the IO, cannot categorically be excluded.

Some data concerning small projection neurons in the cerebellar nuclei may suggest that they form axon branches also outside the cerebellum, the same neuron projecting to the IO and to other regions of the brainstem or thalamus (McCrea et al. 1978; Tolbert et al. 1978; P Brodal, personal communication). Furthermore, some small neurons in the cerebellar nuclei project to the cerebellar cortex (Tolbert et al. 1978; McCrea et al. 1978; Tolbert 1982).

Topography of the cerebello-olivary projection

The topography of the projection from the lateral and interposed nuclei to the IO previously described in the rat (Angaut and Cicirata 1982; Haroian 1982) was confirmed in the present investigation. The lateral cerebellar nucleus projects to the PO and the ventrolateral outgrowth, and the anterior and posterior interposed nuclei project to the DAO and the MAO, respectively.

Small but substantial numbers of GABAergic neurons in the ventrolateral aspect of the medial cerebellar nucleus and the dorsal part of the lateral vestibular nucleus were labeled by HRP injections into the caudal IO. Injections involving the lateral part of the caudal MAO indicate that the medial cerebellar nucleus projects to this region, possibly the subnucleus a, and that the lateral vestibular nucleus projects to the dorsal fold of the DAO. These projections were confirmed by anterograde tract tracing. The existence of projections from the medial cerebellar nucleus and the dorsal lateral vestibular nucleus to the IO have been controversial issues. According to Angaut and Cicirata (1982) and Swenson and Castro (1983a, b) a moderate projection exists in the rat, but Brown et al. (1977) and Haroain (1982) did not observe any contribution from the medial cerebellar nucleus to the IO. A fastigio-olivary projection has been observed in the cat by several investigators (Buisseret-Delmas and Batini 1978; Sugimoto et al. 1980; Dietrichs and Walberg 1981, 1985; Legendre and Courville 1987). Projections from the spinal and medial vestibular nuclei to the caudal IO were described in the rat (Brown et al. 1977; Swenson and Castro 1983a), opossum (Martin et al. 1976) and cat and monkey (Saint-Cyr and Courville 1979; Carleton and Carpenter 1983; Gerrits et al. 1985). A report of a projection from the lateral vestibular nucleus to the IO in rat (Billard et al. 1989) appeared simultaneously with our preliminary report (Nelson and Mugnaini 1989).

Lesion-induced depletion of GAD

The method of depleting GAD enzyme in the IO by destroying the cerebello-olivary axons proved to be a powerful and expedient way to visualize the quantitative importance of this projection. The striking loss of GAD-positive boutons in the major portion of the IO (Fig. 10), namely, the PO, rostral MAO, ventral lateral outgrowth, and lateral portion of the ventral lamella of DAO, after either lesion of the cerebellar nuclei or transection of the superior cerebellar peduncle, demonstrates that most of the IO receives GABAergic afferents almost exclusively from the cerebellar nuclei. The few remaining GABAergic boutons may belong to the few GABAergic neurons identified in the IO territory (Fredette et al. 1991), or to other non-cerebellar afferent systems.

The loss of GABAergic boutons in the dorsal fold of the DAO after destruction of the lateral vestibular nucleus suggests that this olivary region is the target of the GABAergic neurons in the lateral vestibular nucleus. Destruction of the medial cerebellar nucleus by topical lesions (results not shown) failed to produce any visible loss of GABAergic boutons in the IO, and thus, the target boundaries of the GABAergic projection from this nucleus to the IO remain undetermined.

Projections from the lateral and interposed cerebellar nuclei have been previously proven to course in the supe-

rior cerebellar peduncle (Achenbach and Goodman 1968; Graybiel et al. 1973; Haroian 1982; Legendre and Courville 1987). This is consistent with our observation that transection of the superior cerebellar peduncle produces the same effect as cerebellectomy. Since no visible depletion of GAD was observed in the dorsal fold of the DAO after transection of the superior cerebellar peduncle, we speculate that the GABAergic projection from the lateral vestibular nucleus taken a route different from that of the cerebellar projection, but this possibility remains to be clarified.

A previously published study of the GABAergic boutons in the rat IO (Nelson and Mugnaini 1989) revealed that although all olivary regions receive a dense GABAergic innervation, regional differences in bouton size and frequency of occurrence exist. The regions known to receive cerebellar afferents, and which are depleted of GAD-positive boutons after cerebellar lesion, contain the smallest GABAergic boutons in the IO (see also deZeeuw et al. 1988; Angaut and Sotelo 1987). Larger GAD-positive boutons populate the dorsal fold of DAO, and these were depleted after lesions involving the lateral vestibular nucleus. In these two cases, thus, GAD-positive boutons of different sizes belong to GABAergic neurons originating from two different sources. Differences in GAD-positive bouton sizes may be indicative of different sources also concerning other olivary subnuclei.

Olivary regions not affected by lesions of the cerebellar nuclei or lateral vestibular nuclei were the beta nucleus, the dorsal cap, subnuclei a, b, and c of the caudal MAO, the dorsomedial cell column, and a medial region of the ventral fold of the DAO. Only a partial reduction of GABAergic terminals was observed in the rostral tip of the MAO. These regions, therefore, either receive their GABAergic afferents exclusively from non-cerebellar sources, or receive only a partial projection from the cerebellar or lateral vestibular nuclei not detected by our methods. The sources of GABAergic boutons in some of these regions have been identified, and will be described fully in a subsequent paper. Briefly, we have strong evidence that the beta nucleus receives GABAergic input from the spinal vestibular nucleus (Nelson et al. 1986), and that the subnucleus c of the MAO receives a GABAergic input from the parasolitaty nucleus. Also, GABAergic neurons located in the ventral portion of the cuneate nucleus and also outside the ventral border of the nucleus project to the IO, but their termination sites within the IO have not been confirmed. The question of overlapping GABAergic projections may be addressed by anterograde tract-tracing, used in combination with GABA or GAD immunocytochemistry at the EM level.

Concluding remarks

In conclusion, small GABAergic neurons of the cerebellar nuclei and lateral vestibular nucleus, thought by some authors to be local circuit neurons, provide a dense GABAergic, and presumably inhibitory, innervation to a large portion of the IO. GAD immunocytochemistry applied to the IO of the cat, rhesus monkey and human reveal a pattern of GABAergic boutons similar to that observed in the rat (Nelson et al. 1989). Since cerebello-olivary projections also exist in these species (Lapresle and Ben Hamida 1970; Graybiel et al. 1973; Tolbert et al. 1976; Beitz 1976; Kalil 1979), and we have evidence that their cerebellar nuclei also contain small GABAergic neurons, it is likely that the findings of the present study apply not only to the rat, but also to other mammals, as demonstrated for the cat (deZeeuw et al. 1989).

Acknowledgement. This work was supported by USPH grant 00904.

References

Achenbach KE, Goodman DC (1968) Cerebellar projections to pons, medulla and spinal cord in the albino rat. Brain Behav Evol 1:43–57

Adams JC (1981) Heavy metal intensification of DAB-based HRP reaction product. J Histochem Cytochem 29:775

Adams JC, Mugnaini E (1987) Patterns of glutamate decarboxylase immunostaining in the feline cochlear nuclear complex studied with silver enhancement and electron microscopy. J Comp Neurol 262:375–401

Andersson G, Hesslow G (1986) Evidence for an inhibitory action by cerebellar nuclei cells on the inferior olive. Neurosci Lett [Suppl 26]:S231

Andersson G, Hesslow G (1987a) Inferior olive excitability after high frequency climbin fibre activation in the cat. Exp Brain Res 67:523–532

Andersson G, Hesslow G (1987b) Activity of Purkinje cells and interpositus neurones during and after periods of high frequency climbing fiber activation in the cat. Exp Brain Res 67:533–542

Angaut P, Cicirata F (1982) Cerebello-olivary projections in the rat. Brain Behav Evol 21:24–33

Angaut P, Sotelo C (1987) The dentato-olivary projection in the rat as a presumptive GABAergic link in the olivo-cerebello-olivary loop. An ultrastructural study. Neurosci Lett 83:227–231

Beitz AJ (1976) The topographical organization of the olivo-dentate and dentato-olivary pathways in the cat. Brain Res 115:311–317

Billard JM, Batini C, Buisseret-Demas C, Daniel H (1989) The inferior olive innervation from the cerebellar and lateral vestibular nuclei: evidence for a longitudinal zonal segregation of the cortico-nucleo-olivary connection in the rat. In: Strata P (ed) The olivocerebellar system in motor control. Springer, Berlin. Exp Brain Res 17:117–120

Brown JT, Chan-Palay V, Palay SL (1977) A study of afferent input to the inferior olivary complex in the rat by retrograde axonal transport of horseradish peroxidase. J Comp Neurol 176:1–22

Buisseret-Delmas C, Batini C (1978) Topology of the pathways to the inferior olive: an HRP study in cat. Neurosci Lett 10:207–214

Carleton SC, Carpenter MB (1983) Afferent and efferent connections of the medial, inferior and lateral vestibular nuclei in the cat and monkey. Brain Res 278:29–51

Carpenter MB, Nova HR (1960) Descending division of the brachium conjunctivum in the cat: a cerebello-reticular system. J Comp Neurol 114:295–305

Carrea RME, Mettler FA (1955) Function of the primate brachium conjunctivum and related structures. J Comp Neurol 102:151–322

Chan-Palay V (1977) Cerebellar dentate nucleus, organization, cytology, transmitters. Springer, Berlin

Chan-Palay V (1982) Neurotransmitters and receptors in the cerebellum: immunocytochemical localization of glutamic acid decarboxylase, GABA-transaminase, and cyclic GMP and autoradiography with [^{3}H]-muscimol. In: Palay SL, Chan-Palay V (eds) The cerebellum, new vistas. Springer, Berlin, pp 552–584

Chan-Palay V, Palay SL, Wu J-Y (1979) Gamma-aminobutyric acid pathways in the cerebellum studied by retrograde and anterograde transport of glutamic acid decarboxylase antibody after in vivo injections. Anat Embryol 157:1–14

Chen DH (1978) Qualitative and quantitative study of synaptic displacement in chromatolyzed spinal motoneurons of the cat. J Comp Neurol 177:635–664

Cohen D, Chambers WW, Sprague JM (1958) Experimental study of the efferent projections from the cerebellar nuclei to the brainstem of the cat. J Comp Neurol 109:233–259

Cummings SL, Young WS III, Bishop GA, DeSousa EB, King JS (1989) Distribution of corticotropin-releasing factor in the cerebellum and precerebellar nuclei of the opossum: a study utilizing immunohistochemistry, in situ hybridization histochemistry, and receptor autoradiography. J Comp Neurol 280:501–521

Desclin JC (1974) Histological evidence supporting the inferior olive as the major source of cerebellar climbing fibers in the rat. Brain Res 77:365–384

deZeeuw CI, Holstege JC, Calkoen F, Ruigrok TJH, Voogd J (1988) A new combination of WGA-HRP anterograde tracing and GABA immunocytochemistry applied to afferents of the cat inferior olive at the ultrastructural level. Brain Res 447:369–375

deZeeuw CI, Holstege JC, Ruigrok TJH, Voogd J (1989) Ultrastructural study of the GABAergic, cerebellar, and mesodiencephalic innervation of the cat medial accessory olive: anterograde tracing combined with immunocytochemistry. J Comp Neurol 284:12–35

deZeeuw CI, Holstege JC, Ruigrok TJH, Voogd J (1990a) Mesodiencephalic and cerebellar terminals end upon the same dendritic spines within the glomeruli of the cat and rat inferior olive: an ultrastructural study using a combination of [^{3}H]leucine and WGA-HRP anterograde tracing. Neuroscience 34:645–655

deZeeuw CI, Ruigrok TJH, Holstege JC, Jansen HG, Voogd J (1990b) Intracellular labeling of neurons in the medial accessory olive of the cat. II. Ultrastructure of dendritic spines and their GABAergic innervation. J Comp Neurol 300:478–494

deZeeuw CI, Ruigrok TJH, Holstege JC, Schalekanp MPA, Voogd J (1990c) Intracellular labeling of neurons in the medial accessory olive of the cat. III. Ultrastructure of axon hillock and initial segment and their GABAergic innervation. J Comp Neurol 300:495–510

Dietrichs E, Walberg F (1981) The cerebellar nucleo-olivary projection in the cat. Anat Embryol 162:51–67

Dietrichs E, Walberg F (1985) The cerebellar nucleo-olivary and olivo-cerebellar nuclear projection in the cat as studied with anterograde and retrograde transport in the same animal after implantation of crystalline WGA-HRP II. The fastigial nucleus. Anat Embryol 173:253–261

Dietrichs E, Walberg F (1989) Direct bidirectional connections between the inferior olive and the cerebellar nuclei. In: Strata P (ed) The olivocerebellar system in motor control. Springer, Berlin. Exp Brain Res Ser 17:61–81

Flood S, Jansen J (1966) The efferent fibers of the cerebellar nuclei and their distribution on the cerebellar peduncles in the cat. Acta Anat 63:137–166

Fredette BJ, Adams JC, Mugnaini E (1991) GABAergic neurons in the mammalian inferior olive and ventral medulla detected by glutamate decarboxylase immunocytochemistry. J Comp Neurol (in press)

Gerrits NM, Voogd J, Magras IN (1985) Vestibular afferents of the inferior olive and the vestibulo-olivo-cerebellar climbing fiber pathway to the flocculus in the cat. Brain Res 332:325–336

Graybiel AM, Nauta HJW, Lasek RJ, Nauta WJH (1973) A cerebello-olivary pathway in the cat: an experimental study using autoradiographic tracing techniques. Brain Res 58:205–211

Haroian AJ (1982) Cerebello-olivary projections in the rat: an autoradiographic study. Brain Res 235:125–130

Hesslow G (1986) Inhibition of inferior olivary transmission by mesencephalic stimulation in the cat. Neurosci Lett 63:76–80

Houser CR, Barber RP, Vaughn JE (1984) Immunocytochemical localization of glutamic acid decarboxylase in the dorsal lateral vestibular nucleus: evidence for an intrinsic and extrinsic GABAergic innervation. Neurosci Lett 47:213–220

Ito M (1984) The Cerebellum and Neural Control. Raven Press, New York

Kalil K (1979) Projections of the cerebellar and dorsal column nuclei upon the inferior olive in the Rhesus monkey: an autoradiographic study. J Comp Neurol 188:43–62

King JS, Andrezik JA, Falls WM, Martin GF (1976) The synaptic organization of the inferior olivary circuit. Exp Brain Res 26:159–179

Kitai ST, Preston JR, McCrea R (1975) Interposito-olivary and olivo-interpositus relationship: An electrophysiological study. Anat Rec 181:396

Korneliussen HK (1968) On the morphology and subdivision of the cerebellar nuclei of the rat. J Hirnforsch 10:109–122

Krnjevic K (1976) Inhibitory action of GABA and GABA-mimetics on vertebrate neurons. In: Roberts E, Chase TN, Tower DB (eds) GABA in nervous system function. Raven Press, New York, pp 269–281

Lapresle J, Ben Hamida M (1970) The dentato-olivary pathway. Somatotopic relationship between the dentate nucleus and the contralateral inferior olive. Arch Neurol 22:135–143

Legendre A, Courville J (1987) Origin and trajectory of the cerebello-olivary projection: an experimental study with radioactive and fluorescent tracers in the cat. Neurosci 21:877–891

Llinás R (1974) Motor aspects of cerebellar control. Physiologist 17:19–46

Llinás R (1989) Electrophysiological properties of the olivocerebellar system. In: Strata P (ed) The olivocerebellar system in motor control. Springer, Berlin, pp 201–208

Llinás R, Yarom Y (1986) Oscillatory properties of guinea-pig inferior olivary neurones and their pharmacological modulation: an in vitro study. J Physiol (Lond) 376:163–182

Martin GF, Henkel CK, King JS (1976) Cerebello-olivary fibers: their origin, course and distribution in the North American opossum. Exp Brain Res 24:219–236

Matsushita M, Iwahori N (1971) Structural organization of the interpositus and the dentate nuclei. Brain Res 35:17–36

McCrea RA, Bishop GA, Kitai ST (1978) Morphological and electrophysiological characteristics of projection neurons in the nucleus interpositus of the cat cerebellum. J Comp Neurol 181:397–420

Mehler WER (1967) Double descending pathways originating from the superior cerebellar peduncle. An example of neural species differences. Anat Rec 157:374

Mehler WR, Rubertone JA (1985) Anatomy of the vestibular nucleus complex. In: Paxinos G (ed) The rat nervous system. Vol 2 Hindbrain and spinal cord. Academic Press, Sydney, pp 185–219

Mehler WR, Vernier VG, Nauta WJH (1958) Efferent projections from dentate and interpositus nuclei in primates. Anat Rec 130:430–431

Mesulam MM (1978) Tetramethylbenzidine for horseradish peroxidase neurohistochemistry: a non-carcinogenic blue reaction product with superior sensitivity for visualizing neural afferents and efferents. J Histochem Cytochem 26:106–116

Monaghan PL, Clements JR, Madl JE, Maley BE, Larson AA, Beitz AJ (1986a) Ultrastructural analysis of GABAergic and glutaminergic cells and processes in the deep cerebellar nuclei of the rat. Soc Neurosci Abstr 12:462

Monaghan PL, Bietz AJ, Larson AA, Altschuler RA, Madl JE, Mullett MA (1986b) Immunocytochemical localization of glutamate-, glutaminase- and aspartate aminotransferase-like im-

munoreactivity in the rat deep cerebellar nuclei. Brain Res 363:364–370
Mugnaini E, Nelson BJ (1989) Corticotropin-releasing factor (CRF) in the olivocerebellar system and the feline olivary hypertrophy. Exp Brain Res Ser 17:187–190
Mugnaini E, Oertel W (1981) Distribution of glutamate decarboxylase positive neurons in the rat cerebellar nuclei. Soc Neurosci Abstr 7:122
Mugnaini E, Oertel WH (1985) An atlas of the distribution of GABAergic neurons and terminals in the rat CNS as revealed by GAD immunocytochemistry. In: Björklund A, Hökfelt T (eds) Handbook of chemical neuroanatomy, Vol 4: GABA and Neuropeptides in the CNS, Part I. Elsevier, British Vancouver, pp 436–608
Nelson B, Mugnaini E (1985) Loss of GABAergic nerve terminals in the inferior olive of cerebellectomized rats. Soc Neurosci Abstr 11:182
Nelson BJ, Mugnaini E (1988) The rat inferior olive as seen with immunostaining for glutamate decarboxylase. Anat Embryol 179:109–127
Nelson BJ, Mugnaini E (1989) Origins of GABAergic inputs to the inferior olive. In: Strata P (ed) The oivocerebellar system in motor control. Springer, Berlin. Exp Brain Res Ser 17:86–107
Nelson B, Barmack NH, Mugnaini E (1984) A GABAergic cerebello-olivary projection in the rat. Soc Neurosci Abstr 10:539
Nelson B, Barmack NH, Mugnaini E (1986) GABAergic projection from vestibular nuclei to rat inferior olive. Soc Neurosci Abstr 12:225
Nelson BJ, Adams JC, Barmack NH, Mugnaini E (1989) A comparative study of glutamate decarboxylase immunoreactive boutons in the mammalian inferior olive. J Comp Neurol 286:514–539
Oertel WH, Schmechel DE, Tappaz ML, Kopin IJ (1981a) Production of a specific antiserum to rat brain glutamic acid decarboxylase by injection of an antigen-antibody complex. Neuroscience 6:2689–2700
Oertel WH, Schmechel DE, Mugnaini E, Tappaz ML, Kopin IJ (1981b) Immunocytochemical localization of glutamate decarboxylase in rat cerebellum with a new antiserum. Neuroscience 6:2715–2735
Oertel WH, Schmechel DE, Brownstein MJ, Tappaz ML, Ransom DH, Kopin IJ (1981c) Decrease of glutamate decarboxylase (GAD)-immunoreactive nerve terminals in the substantia nigra after kainic acid lesions of the striatum. J Histochem Cytochem 29:977–980
Ohkawa K (1957) Comparative anatomical studies of cerebellar nuclei in mammals. Arch Hist Jpn 13:21–58
Ottersen OP, Storm-Mathisen J (1984) Glutamate- and GABA-containing neurons in the mouse and rat brain as demonstrated with a new immunocytochemical technique. J Comp Neurol 229:374–392
Peters A, Palay SL, Webster H deF (1991) The fine structure of the nervous system: neurons and their supporting cells, 3rd edn. Oxford University Press, New York Oxford
Ramon Y, Cajal S (1911) Histologie du système nerveux de l'homme et des Vertébrés, Vol I. Maloine, Paris
Ribak CE, Vaughn JE, Roberts E (1980) GABAergic nerve terminals decrease in the substantia nigra following hemitransection of the striatonigral and pallidonigral pathways. Brain Res 192:413–420
Saint-Cyr JA, Courville J (1979) Projection from vestibular nuclei to the inferior olive in the cat: an autoradiographic and horseradish peroxidase study. Brain Res 165:189–200
Sasaki K, Llinás R (1985) Dynamic electrotonic coupling in mammalian inferior olive as determined by simultaneous multiple Purkinje cell recording. Biophys J 47:53a
Sotelo C, Gotow T, Wassef M (1986) Localization of glutamic-acid-decarboxylase-immunoreactive axon terminals in the inferior olive of the rat, with special emphasis on anatomical relations between GABAergic synapses and dendro-dendritic gap junctions. J Comp Neurol 252:32–50
Sugimoto T, Mizuno N, Nomura S, Nakamura Y (1980) Fastigio-olivary fibers in the cat as revealed by the autoradiographic tracing method. Brain Res 199:443–446
Swenson RS, Castro AJ (1983a) The afferent connections of the inferior olivary complex in rats: a study using the retrograde transport of horseradish peroxidase. Am J Anat 166:329–341
Swenson RS, Castro AJ (1983b) The afferent connections of the inferior olivary complex in rats. An anterograde study using autoradiographic and axonal degeneration techniques. Neuroscience 259:275
Tolbert DL (1982) The cerebellar nucleocortical pathway. In: Palay SL, Chan-Palay V (eds) The cerebellum: new vistas. Springer, Berlin, pp 296–317
Tolbert DL, Bantli H (1980) Uptake and transport of ^{3}H-GABA (γ-aminobutyric acid) injected into the cat dentate nucleus. Exp Neurol 70:525–538
Tolbert DL, Massopust LC, Murphy MG, Young PA (1976) The anatomical organization of the cerebello-olivary projection in the cat. J Comp Neurol 170:525–544
Tolbert DL, Bantli H, Bloedel JR (1978) Multiple branching of cerebellar efferent projections in cats. Exp Brain Res 31:305–316
Tolbert DL, Bantli H, Hames EG, Ebner TJ, McMullen TA, Bloedel JR (1980) A demonstration of the dentato-reticulospinal projection in the cat. Neuroscience 5:1479–1488
Wiklund L, Toggenburger G, Cuenod M (1982) Aspartate: possible neurotransmitter in cerebellar climbing fibers. Science 216:78–79